NEW DESIGNED THIOL POLYMERS AND POLYAMINE/CNT COMPOSITES FOR TOXIC HEAVY METAL ION REMOVAL

BY

Muhammad Alasad Albakri

A Thesis Presented to the

DEANSHIP OF GRADUATE STUDIES

KING FAHD UNIVERSITY OF PETROLEUM & MINERALS

DHAHRAN, SAUDI ARABIA

In Partial Fulfillment of the

Requirements for the Degree of

MASTER OF SCIENCE

In

CHEMISTRY

November 2018

KING FAHD UNIVERSITY OF PETROLEUM & MINERALS

DHAHRAN- 31261, SAUDI ARABIA

DEANSHIP OF GRADUATE STUDIES

This thesis, written by **Muhammad Alasad Albakri** under the direction of his thesis advisor and approved by his thesis committee, has been presented and accepted by the Dean of Graduate Studies, in partial fulfillment of the requirements for the degree of **Master of Science in Chemistry**

Dr. Othman Al-Hamouz
(Advisor)

Dr. Khalid Al Hooshani
Department Chairman

Dr. Tawfik A. Saleh
(Member)

Prof. Salam A. Zummo
Dean of Graduate Studies

Dr. Thomas F. Garrison
(Member)

13/1/19

Date

ACKNOWLEDGMENTS

First and foremost, unlimited gratitude to Allah where no achievement can be done without his will, Alhamdulillah! For everything.

To my beloved parents with their support, prayers and encouragement, to my brothers and sister, and to my great wife and kids with thankfulness.

To my friends, colleagues and classmates who shared with me their knowledge, experience and support.

To the KFUPM chemistry department faculty who taught me and gave me unpaid back support, and to all the department technicians for their dedication and help.

To my great advisor Dr. Othman Alhamouz, for his guidance and patience. I learned much from him and there are no words to describe my respect to him. To the committee members Dr. Tawfik Saleh and Dr. Thomas Garrison for their support.

To my best friend, my colleague, my teammate and my inspiration Asem Zino.

Finally to all the people who supported me in completing this study and make my dream a reality, Thank you indeed!

TABLE OF CONTENTS

LIST OF TABLES

LIST OF FIGURES

ABSTRACT

Full Name : [Muhammad Alasad Albakri]

Thesis Title : [New designed thiol polymers and polyamine/CNT composites for toxic heavy metal ion removal]

Major Field : [Master of Science in Chemistry]

Date of Degree : [December 2018]

In this study, a new series of polymers have been synthesized using different aliphatic diamines and benzene 1,3,- triamine in presence of paraformaldehyde. This series was subsequently modified with multi walled nanotubes (MWCNT) to have another series of polymers. Both series (TRI and CNT TRI) were characterized using different techniques including, nuclear magnetic resonance spectroscopy (NMR), Fourier transform infrared spectroscopy (FTIR) and elemental analyzer. The thermal behavior were studied by differential scanning calorimetry (DSC) and thermogravimetric analysis (TGA). The morphology and composition were determined using scanning electron microscopy coupled with energy dispersive X-ray (SEM-EDX). Crystallinity of the polymers was investigated using X-ray diffraction (XRD).

Both series of polymers were studied to evaluate their ability to remove lead ions from aqueous solution. The best polymer of each series was subjected to further study on lead ion removal under different conditions of pH, contact time and lead concentration in order to understand the mechanism and behavior of these polymers as a potential adsorbents for the toxic lead ions from wastewater.

The second part of this study was performed by synthesizing a different type of polymer via Freidel craft alkylation using pyrrole and thiophenol with paraformaldehyde,

which can be also used for mercury ion removal. This polymer was found to have a high surface area during characterization using similar techniques used for the previous polymers, therefore it was further studied for CO_2 and H_2S capture from natural gas. The results were considered rewarding compared to the conventional known sorbents. Porosity experiments showed the material was mesoporous. The breakthrough isotherms showed a high selectivity towards CO_2 and H_2S gases in a natural gas stream. The adsorption capacity, stability and ability for regeneration of the polymer were also studied, and the results showed this is a promising new polymer for CO_2 and H_2S removal compared to a currently reported materials in the literature.

ملخص الرسالة

الاسم الكامل: محمد الأسعد البكري

عنوان الرسالة: بوليميرات الثيو جديدة التصميم ومركبات البولي أمين/أنابيب الكربون النانوية لإزالة إيونات المعادن الثقيلة السامة

التخصص: كيمياء

تاريخ الدرجة العلمية: ديسمبر 2018

في هذه الدراسة، تم تصنيع سلسلة جديدة من الوليميرات باستخدام ألكينات ثنائية الأمين و مركب ثلاثي أمين البنزن بوجود مادة البارافورم ألدهيد، ثم تم تعديل تركيبة سلسلة البوليميرات الناتجة باستخدام مادة انابيب الكربون النانوية لتشكيل سلسلة مطورة من البوليميرات، تم بعد ذلك عملية توصيف لهذه البوليميرات باستخدام عدة تقنيات تتضمن الرنين النووي المغناطيسي و طيف الاشعة تحت الحمراء وجهاز تحليل العناصر، السلوك الحراري تمت دراسته بواسطة مسعر المسح التباييني و جهاز التحليل الحراري الوزني. دراسة التشكيل والتركيب تمت بواسطة المجهر الإلكتروني مقترن ب مطيافية تشتت الطاقة بالأشعة السينية، أما صفات تبلور البوليميرات فقد تمت بواسطة جهاز أشعة الحيود السينية.

كلا السلسلتين من البوليميرات المصنعة تمت دراسة قدرتها على إزالة إيونات معدن الرصاص من المحاليل المائية، بعد ذلك أجريت دراسات أخرى على أفضل بوليمير من كل سلسلة لإزالة أيونات الرصاص تحت ظروف مختلف من الأس الهيدروجيني و زمن التماس بين البوليمر والمحلول المحتوي على الرصاص بالإضافة إلى تراكيز مختلفة من إيونات الرصاص لفهم ألية عمل هذه البوليميرات وسلوكها كمواد ذات قابلية على امتزاز إيونات الرصاص السامة من مياه الصرف الصحي.

في القسم الثاني من هذه الدراسة، تم تصنيع نوع جديد من البوليميرات باستخدام ألية فريديل-كرافت لمفاعلة مادة البيرول مع مادة الثيوفينول وبوجود مادة البارافورم ألدهيد للحصول على بوليمر يمكن استخدامه في إزالة إيونات الزئبق من مياه الصرف الصحي، ,اثناء اختبارات التوصيف لهذا البوليمر الجديد، تمت ملاحظة أن المساحة السطحية لهذا البوليمر عالية نسبيا، لذلك تم إجراء عدة تجارب على هذا البوليمر كمادة قادرة على امتزاز غازي ثاني أوكسيد الكربون و كبريتيد الهيدروجين، وقد كانت النتائج مثيرة للإهتمام عند مقارنتها بالمواد التقليدية المستخدمة في هذا

المجال، وقد أجريت أيضا تجارب لمعرفة الخصائص المسامية للمادة، وأظهرت دراسة منحنيات الفصل انتقائية عالية لغاز ثاني أوكسيد الكربون وغاز كبريتيد الهيدروجين تيار الغاز الطبيعي، تمت أيضا دراسة سعة الامتزاز و الثباتية و قابلية إعادة تنشيط هذا البوليمر، النتائج كانت مبهرة بتفوق هذا البوليمر على المواد الموجودة في اوراق البحث المنشورة سابقا في نفس هذا المجال.

CHAPTER 1

INTRODUCTION

Many types of pollution are negatively affecting the environment in our modern industrial life. The pollutants can be caused by the discharge from industrial sources or from other human activities, and the contamination coming from these pollutants is mixed with water, soil, and air. Because of the toxicity of these contaminants, it has become a critical challenge for scientists to find a solutions to eliminate the severe health impact on human and on other living organism [1,2].

Several sources of pollutants are affecting water quality include domestic waste, industrial waste disposal, leaching of fertilizers into the ground water, pesticides and herbicides. The sources contaminate the water with heavy metals, hydrocarbons, and other toxic chemicals. Sources of soil pollution include acid rain, solid waste disposal, and garbage [2,3].

Likewise, air is also exposed to pollution by different gases, (e.g nitrogen and sulfur oxides), and volatile organic materials and carbon oxides, that are primarily produced from combustion of gas, oil, and coal in industrial processes [4,5].

In this study, we will compare the conventional methods for the removal of certain air and water pollutants with the results by the new synthesized polymers.

1.1 Water Pollution

Water pollution is one of the most urgent environmental concerns causing significant problems worldwide to human beings and living organism. Finding solutions for removal of different toxic contaminants from water streams and wastewater effluent has been a major interest for academic and industrial researchers in many research and development centres globally. The goal of researchers is to remove the inorganic and organic toxic materials form the wastewater; heavy metals are part of these dangerous materials because of its high toxicity and availability, it is causing serious health issues for human being, animals and marine life.

Many industries are contributing to water pollution such as mining, steel industries, metal finishing, dye and pigments, battery manufacturing, as well as many other sectors that generate toxic materials in the wastewater discharge [6,7]. The optimum solution for preventing damage to the ecosystem is to remove the pollutants from the waste before discharging them into the environment [8].

Heavy metals like nickel (Ni), lead (Pb), cadmium (Cd), mercury (Hg), arsenic (As), and chromium (Cr) are the major toxic inorganic contaminants that polluting water due to their presence in fertilizers, sludge, domestic waste, and metal alloys industries [9]. Heavy metals are non-degradable, carcinogenic agents that cause serious health problems for living organisms due to the accumulative and persistent nature [10–12]. Although, some heavy metals are necessary for human and play an important role in the metabolic process if it did not exceed the required level [13]. Heavy metals are considered to be xenobiotics which are not beneficial for living organisms. Trace levels of these metals cause serious disorders, therefore, international standards have set permissible levels for each heavy

metal in water to be used in drinking water, **Figure 1.1** shows the acceptable level for some heavy metals in accordance to World Health Organization (WHO), US Environmental Protection Agency (US EPA) and European Union (UN) standards [14–16].

Many techniques were developed globally in order to minimize and control the hazard of the heavy metals in wastewater like, evaporation, chemical precipitation, and adsorption, membrane filtration technologies, oxidation, ion exchange, coagulation, flocculation and electrochemical treatment [17–22].

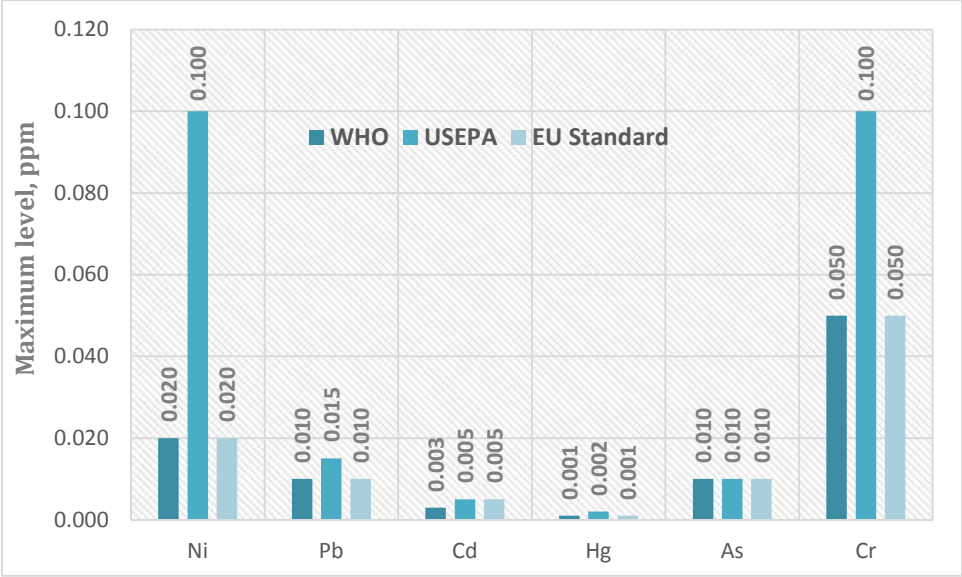

Figure 1.1 Drinking water guidelines for some heavy metals in accordance to different standards

While each method has its own advantages and disadvantages, the application of chemical precipitation using hydroxide (OH^-) and sulphide (S^{-2}) is a particularly efficient conventional method because of its ease process and the economical capital cost. However, chemical precipitation is only effective for high concentrations of heavy metal ions and is not suitable for removal at low concentrations of heavy metals. Furthermore chemical

precipitation generates huge amount of contaminated sludge with the potential risk of releasing toxic hydrogen sulphide (H_2S) fumes, which is another type of pollution [23–25]. While membrane filtration with different membrane types has high efficiency, simple operation, and low footprint requirements, this technique is not cost-effective compared to other techniques due to the high cost of membranes that must be changed frequently [26].

Ion exchange is an expensive technique that cannot be feasibly used for massive wastewater stream due to the huge requirement, for resin regeneration which needs a considerable amount of regeneration chemicals, and the generating of secondary chemical waste stream [27]. Electrochemical methods have limited use because of the elevated electrical consumption and the large capital cost required for the plant [28]. Coagulation and flocculation process are efficient to remove suspended solids and hydrophobic contaminants, but cannot be used for the removal of heavy metal ions without incorporating other technologies like filtration or sedimentation [29]. New adsorption process show significant advantages in contrast to all these other techniques for the removal of heavy metals from wastewater. Some of these advantages are the availability of many types of adsorbents, low-cost, ease of operation, and excellent removal efficiency, which made adsorption a promising technology to wash out heavy metals from wastewater [30,31].

The principle of adsorption can be explained as a surface phenomenon that happen as a result of chemical interaction or physical forces. Adsorption kinetics and isotherms are key Figures characteristics that define the adsorption uptake rate; they indicate the adsorbent efficiency and the adsorption parameters [32].

Lead is a toxic heavy metal that considered as a major contaminant of water. Lead (Pb^{+2}) contamination in wastewater and drinking water is a serious concern because of the deleterious effect on human and animal health if ingested. Persistent exposure to lead, even at trace levels, can create long term illness and health problems. Lead ions (Pb^{+2}) cannot be easily excreted from human bodies and will accumulate in the lymphatic system, bones, and digestive system [33, 34]. When lead ions accumulate in the body at high levels, it will cause a lot of maladies such as cancer, fatigue, nerve damage, reduction of male reproductive ability, anemia and digestive troubles [35-37]. Children are more susceptible to the toxic effects of lead, as many studies have shown that abnormal levels of lead can cause mental retardation and impair brain development causing learning difficulties and reduced cognitive skills. Lead is also known to be toxic for plants and animals as well [38-40].

Lead contaminates water streams due to natural and man-made sources. The natural sources of lead include sea aerosols, volcanic eruption and forest fires, while the industrial sources are mainly from lead acid batteries, pigments, thermal power plants using coal as a source of energy, smelting processes and ceramics production. [41].

While several methods are used to remove lead to reach acceptable levels, adsorption is the most common used technique due to many advantages including, cost effective and simple operation. Many adsorbents have been studied for the efficiency of removal of lead from industrial wastewater such as activated carbon, zeolites, clays, bio-sorbents, carbon nanotubes and nano sized metal oxides [42-45].

In this study, we will discuss the use of a new series of benzene-1,3,5-triamine based cross-linked polyamines and polyamine/carbon nanotubes (CNT) composites as new adsorbents for lead ion removal from aqueous solutions.

1.2 Air Pollution

Air pollution is one of the major dangerous health risks to humans worldwide. Recently reported data from the (WHO) shows that 90% of people are breathing contaminated air with high levels of pollutants and this invisible killer leads to seven million death yearly [46].

Anthropogenic climate change which is known as global warming is occurring as a result of the elevated emission of the greenhouse gases since the Industrial Revolution.

The main contribution of greenhouse gases is carbon dioxide (CO_2), along with other gases like nitrous oxide methane, and fluorinated gases. **Figure 1.2** shows the distribution of greenhouse gases according to the US EPA. Because of greenhouse gases, the temperature of the earth has increased 1.8 °F according to the National Aeronautics and Space Administration (NASA), and it is expected that temperature will continue to increase during the 21st century [47-49].

Global warming causes many serious problems across the planet. It is leading to droughts, demolition of the ecosystem, floods, and heat waves, in addition to an economic loss between 5-20% of gross domestic product (GDP) worldwide as a result of climate change [50,51].

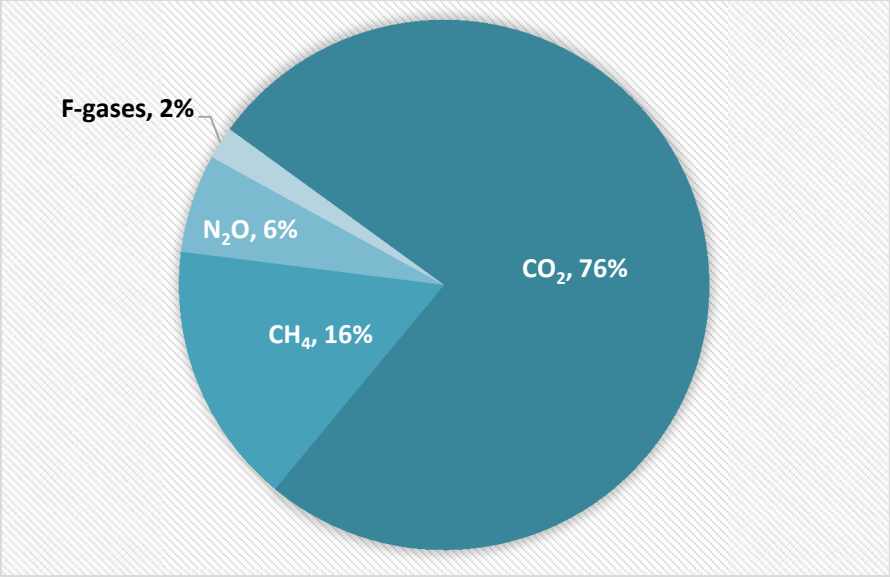

Figure 1.2 Global Greenhouse gases distribution

Carbon dioxide is the primary greenhouse gas and major cause of global warming. 15% of CO_2 emissions have natural sources, while 85% is due to human activities such as transportation, power generation plants, and other industrial plants. **Figure 1.3** illustrate the distribution of CO_2 emission by sectors as classified by US EPA. Because of the huge emission from industrial plants, the concentration of CO_2 is continuing to increase. According to the International Energy Agency (IEA), global atmospheric carbon dioxide has been increased by 40% in 2012 with major emissions from fossil fuels combustion [52,53].

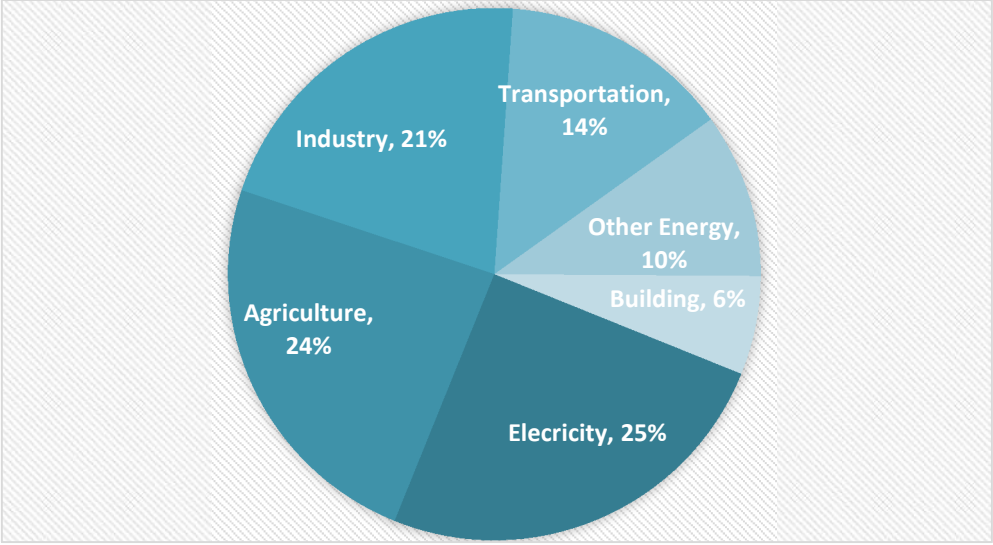

Figure 1.3 Greenhouse gases by sectors

According to US EPA, the United States of America and China are producing 45% of total CO_2 emissions in the world. **Figure 1.4** presents the top ten countries in terms of CO_2 emissions in million metric tons (MMT) for 2014 [54].

Serious efforts are being undertaken at implementing strict regulations of CO_2 emissions due to the increased of awareness of environmental concerns. In 1997, the United Nations helped in making a landmark international agreement, the Kyoto Protocol, with the goal to reduce greenhouse gas emissions. As a result, these has been increased interest in finding new techniques that reduce CO_2 generation rates, as well as significant attention to post treatment of CO_2 [55,56].

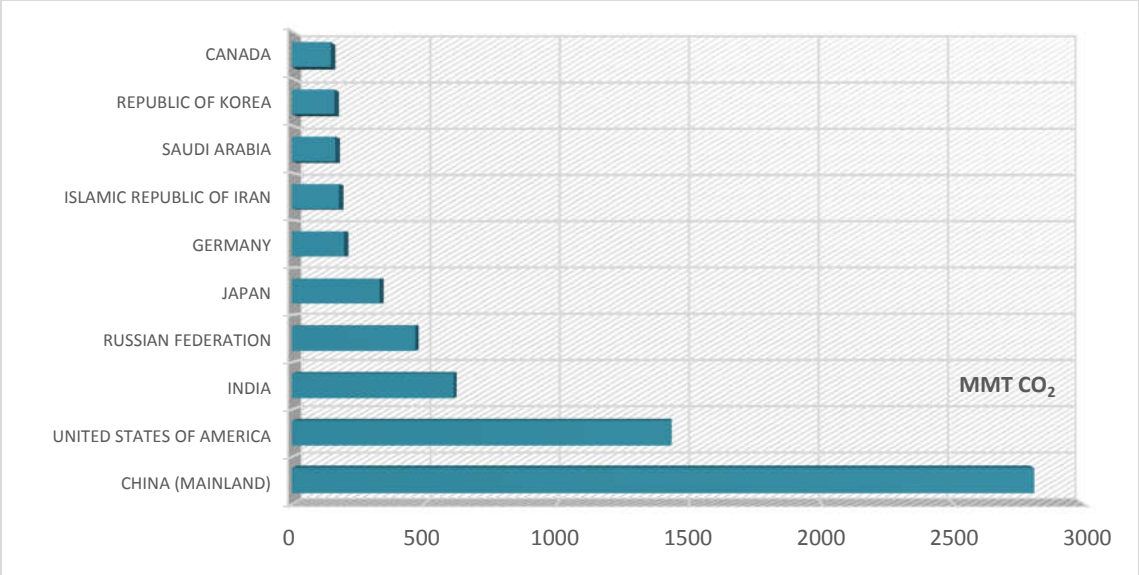

Figure 1.4 CO_2 emission from main industries by country

The best solution for lowering CO_2 levels in the atmosphere is cleaner industrial processes and environmentally friendly energy sources, but practically, this solution cannot be achieved easily in the near future [57]. Many other options do exist to minimize CO_2 emissions, such as increasing dependence on renewable energy and nuclear power plants in reducing demand, improving the supply efficiency, and implementing carbon capture and storage (CCS) process [58,59]. The capture of CO_2 is most efficient when applied directly on-site where CO_2 level concentrations are high [60].

Gas adsorption on a solid adsorbent is done by gaining a number of gas constituents or adsorbate on the surface of the adsorbent. Adsorption methods can decrease the cost and energy needed to separate CO_2 gas in the post-combustion capture method [61]. CO_2 adsorption by solid adsorbents is one of the promising technologies for CCS processes [62]. However, to implement this approach successfully, developing new durable adsorbents that can be recoverable easily and have high adsorption capacity and significant selectivity for CO_2 is essential [63].

Some of the common conventional adsorbents for CO_2 are alkali-based metal compounds, natural zeolites, mesoporous silica, and activated carbon, but these adsorbents typically have limitations of low adsorption capacity and low selectivity [64-66]. This has driven the researchers to develop new advanced adsorbents that have better characteristics comparing to the existing conventional materials.

Proper sorbent selection remains a problematic issue, thus, number of criteria have been considered while developing new sorbents to have operational and economical CO_2 capture [67-70]. The main criteria include:

1. Adsorption capacity is one of the most important criteria. It has a great impact on the capital cost of the CO_2 capture system because it defines the amount of required sorbent and therefore the volume of the adsorbent vessels. The higher adsorption capacity, the lower sorbent quantity and vessel size is required [71].

2. Selectivity for the adsorbate (CO_2) is defined as the ratio of CO_2 capacity against another gas at known flue gas composition. For example, since methane (CH_4) is often present along with CO_2 in gaseous mixtures, like natural gas and landfill gas, selectivity will play an important role in improving the energy content of gas mixture. Furthermore the purity of the adsorbed CO_2 will have impact on sequestration and transportation [72].

3. Adsorption and desorption kinetics are essential to the selection of a good adsorbent. The faster the CO_2 adsorption/desorption under the operational conditions, the better the performance. In other words, an adsorbent that has a fast CO_2 adsorption and desorption

needs less cycle time which means it will capture higher volume of CO_2 in the flue gas [73].

4. Mechanical strength: The sorbent particle should have high stability for its morphology and microstructure. This will help in retaining CO_2 adsorption capacity over multicycling process (absorption and regeneration). High mechanical strength for the sorbent under operational conditions such as temperature, flue gas flow rate, and vibration will minimize the makeup rate of sorbent and will make the CO_2 capture process more cost-effective [73].

5. Chemical stability is another important criteria to be considered while choosing an adsorbent. Solid CO_2 adsorbents, particularly adsorbents based on functionalized amines, must be stable under the oxidizing conditions of flue gas and should be resistant against flue gas contaminants such as NOx, SOx and heavy metals as these contaminant will negatively affect the adsorption capacity for CO_2 [74].

6. Regeneration is a key factor for efficient sorbents, and the required energy required for regeneration should be very low. Heats of adsorption for physisorption method are generally between 25 and 50 kJ/mol, while in chemisorptions cases it is found to be between 60 and 90 kJ/mol. The new sorbents that can be easily regenerated while maintaining sorption capacity will help facilitate more cost effective process [73].

7. Finally, the sorbent cost will play an important role for the feasibility of sorbent, previous techno economic analysis were used an approximate baseline of $10/kg for the

sorbent for an economic performance, Therefore, to have an economical sorbent for CO_2 capture, the cost of it below $10/kg [75].

Ideally it will be preferred to have a sorbent that fulfil all of the listed criteria, although in reality sorbent should have an acceptable balance of all criteria.

Although hydrogen sulfide (H_2S) pollution is smaller in magnitude compared to CO_2, H_2S is a highly toxic gas and flammable in nature. H_2S is colorless gas that has a characteristic rotten eggs odor. Since H_2S has higher density than air, it tends to settle down in low ventilation areas. H_2S causes irritation to the nose, eyes and throat at even low concentrations around 5 ppm, it is also fatal at concentration above 1000 ppm [76,77].

Inhalation is the major route for H_2S exposure. At level of 30 ppm, H_2S paralyzes the smell sense. It will absorbed by the blood rapidly causing low oxygen uptake, thus smell sense should not be trusted while handling H_2S gas.

H_2S may form naturally at different concentration from various sources such as natural gas, biogas, and crude petroleum, natural gas, biogas, landfills and microbiological reactions like respiration of anaerobic sulphate reducing bacteria (SRB) [78-80]. However, H_2S is also formed also as by product during some industrial processes. Sweetening of natural gas is one of these processes which is used for the removal of the acidic sulfur components, mainly H_2S, from natural gas. The US EPA classifies natural gas with H_2S levels of more than 4 ppm as a sour gas [81].

The natural gas coming from the reservoir well are subjected to a low temperatures to remove the heavy hydrocarbons by condensation. The vapours are then sent to sweetening process to remove CO_2 and H_2S acid gases. The stream rich in H_2S is then sent to sulphur

recovery unit (SRU) to recover sulphur via the Claus process (thermal oxidation at high temperatures up to 1000 °C). However, H_2S cannot be conserved completely in the (SRU), therefore some of H_2S stream is released to the atmosphere causing air pollution [82].

H_2S removal methods can be categorized into four types: cryogenic distillation, membranes separation, absorption and adsorption [83-85]. Adsorption technologies for the removal of H_2S have many advantages compared to the others such as effective cost as mentioned earlier. The current conventional materials are most commonly used for H_2S removal are metal oxides, metals, metal organic frameworks, MOF's, zeolites, and activated carbon. New composite materials are subjected to many researches in order to develop better solution for H_2S removal [86].

CHAPTER 2

New Series of Benzene-1,3,5-Triamine Based Cross-Linked Polyamines and Polyamine/Composites for Lead Removal from Aqueous Solutions

Abstract

For the first time, a new series of polyamines were synthesized by in-situ polymerization of benzene-1,3,5-triamine, paraformaldehyde and various alkydiamines (***TRI*** series). 1% of acylchloride functionalized carbon nanotubes were added to produce a second series of polyamine/CNT composites (***CNT TRI*** series). The synthesized TRI and CNT TRI Series were characterized using various techniques including Fourier transform infrared spectroscopy, powder x-ray diffraction, scanning electron microscope (SEM) equipped with energy-dispersive X-ray spectroscopy (EDX). The functionalized CNTs were characterized by transmission electron microscope (TEM). Both series were evaluated for their efficiency in the removal of lead ions from aqueous solutions. The most efficient adsorbent of both series was evaluated under different controlled conditions, including pH, contact time and initial concentration. The experimental data were subjected to Langmuir, Freundlich, and Temkin isotherm models and found that the adsorption process fit Freundlich isotherm model assuming favorable heterogeneous adsorption process with ***CNT TRI 1,4*** having a higher adsorption capacity toward lead ions than ***TRI 1,4***. Kinetic

models including pseudo second-order and intraparticle diffusion model were also employed. The intraparticle diffusion model assumed that the mechanism of the adsorption process is controlled by film diffusion and intraparticle diffusion mechanism. The study provides potential adsorbents for the removal of lead ions from aqueous solutions.

Keywords: polyamine**;** polyamine/CNT composite; lead; adsorption

2.1 Introduction

The presence and toxic effects of pollutants in water bodies have been identified as a global challenge [87]. The presence of pollutants in the environment can be attributed to both natural and anthropogenic sources [88,89]. Heavy metal ions are non-biodegradable pollutants accumulated in groundwater and on the soil surface as a waste of some industrial processes such as; mining, painting, and anti-corrosive coating. The main anthropogenic sources to release lead into natural waters include used batteries, lead smelting, tetraethyl lead industries, mining, plating and ceramic glass industry. According to Environmental Protection Agency, the maximum limit for lead in waters is less than 0.1 mg/L. Higher quantities of lead in fresh water may pose health risks and an increase in diseases, like encephalopathy and hepatitis [90-92].

Therefore, to overcome the problems caused by pollutants, more efforts are required to minimize the impact on the environment. Different removal methods have been adopted in the treatment of lead (II) contaminated waters that include nanofiltration, lime-softening, adsorption, reverse osmosis, coagulation, electrocoagulation, ion exchange,

chemical precipitation [93]. Adsorption is considered a promising method, relying on the efficiency of the sorbent materials. The use of water-insoluble solid adsorbents have been found to be efficient because of their ease of phase separation and high enrichment efficiency [94, 95]. Many physicochemical treatments have been used to adsorb lead (II) from aqueous solution, such as adsorption, ion – exchange, and membrane technology [97]. However, the use of carbon nanotubes (CNT) which has a variety of structural and chemical characteristics loading onto polymers such as benzene-1,3,5-triamine-alkydiamine cross-linked polymers as a sorbent to remove lead ions from aqueous solution has not yet been studied. Designing an appropriate and efficient adsorbent for specific pollutants is the key step for a successful adsorption process. Thus, it is the first time that the series of polymers and their counter polymer/CNT composites have been synthesized and characterized using various techniques including Fourier transform infrared spectroscopy, Scanning electron microscope (SEM), and energy-dispersive X-ray spectroscopy (EDX). The polymers and polymer/CNT composites were evaluated as adsorbents for the removal of lead from aqueous solutions. The effect of several parameters including pH, contact time and initial concentration was investigated and analyzed.

2.2 Experimental

2.2.1 Material and Methods

Benzene-1,3,5-triamine trihydrochloride (**TRI**), paraformaldehyde, 1,4-diaminbutane (**1,4**), 1,6-diaminohexane (**1,6**), 1,8-diaminooctane (**1,8**) and 1,10-diaminodecane (**1,10**) from Fluka Chemie AG (Buchs, Switzerland) were used as received. All solvents used were of analytical grade. Infrared spectra were recorded on a Perkin Elmer 16F PC FTIR in the 500 - 4000 cm-1 region (FT-IR). Thermogravimetric analysis (TGA) was performed

using a thermal analyzer (STA 429) by Netzsch (Germany). X-ray analysis was performed on Rigaku Rint D/max – 2500 diffractometer using Cu Kα radiation (wave length = 1.5418 A) in a scanning range 2θ = 5 – 50 degree. For lead ion concentration determination before and after adsorption; inductively coupled plasma- mass spectroscopy (ICP-MS) analysis was performed using ICP-MS XSERIES-II (Thermo Scientific). The surface morphology of the chosen polymer and polymer/CNT composite was characterized by scanning electron microscopy (TESCAN LYRA 3, Czech Republic) equipped with an energy-dispersive X-ray spectroscopy (EDX) detector model X-Max. Morphological analysis of the CNT was performed using FEI Titan 300, transmission electron microscope (TEM), operated at 120 kV. The sample preparation was performed by dispersing CNT in ethanol, which was followed by deposition of an air-dried sample on a carbon coated grid for TEM analysis.

2.2.2 Synthesis of functionalized CNT

The acyl cholride functionalized CNT was synthesized and functionalized in a similar way as reported in the literature [98]. Briefly, the CNT was prepared by the chemical vapor deposition reactor using ferrocene as a source of iron catalyst. Acetylene gas was used as a hydrocarbon source and hydrogen gas as a carrier and a reactant gas while argon was used to flush the air from the system before and after the completion of the reaction. The obtained CNT was treated with nitric acid at 120 ^{o}C for 6h for creating carboxylic groups. The activated Carbon nanotubes (CNT) (5% COOH) were refluxed in excess thionyl chloride for two hours then filtered and dried.

2.2.3 Synthesis of benzene-1,3,5-triamine based polyamine and polyamine/CNT composite

The following procedure was conducted to synthesize the polyamines (***TRI*** series): benzene-1,3,5-triamine (0.01 mol), diaminoalkane (0.03 mol) and paraformaldehyde (0.06 mol) were added to 20 ml DMF and stirred at 90°C for 24 hours to produce a reddish brown solid, once cooled down the solid was washed several times with methanol and dried at 60°C until constant weight was achieved [99].

For the synthesis of the CNT TRI series CNT (1 % wt. of all reactants) was added to 20 ml DMF followed by the diaminines, then the benzene-1,3,5-triamine and finally the paraformalehyde. The solution mixture was stirred at 90°C for 24 hours to produce a black solid powder to form the polyamine/CNT composites (***CNT TRI*** series).

Table 2-1

Polymer	Yield %*	Polymer/CNT composite	Yield %*
TRI 1,4	76	***CNT TRI 1,4***	82
TRI 1,6	62	***CNT TRI 1,6***	84
TRI 1,8	69	***CNT TRI 1,8***	79
TRI 1,10	71	***CNT TRI 1,10***	86

*Yield (%) = (mass of product/mass of reactants)×100%.

Table 2-1 Results for the synthesis of *TRI* and *CNT TRI* series

2.2.4 Adsorption experiments

At first, the ***TRI*** and ***CNT TRI*** series were evaluated in order to determine the most efficient polymer and polymer/CNT composite toward the removal of lead ions from

aqueous solutions. The most efficient polymer is then further tested as follows: in a typical experiment; 0.03 g polymer sample was inserted into a 20 ml metal ion solution at a specified condition (pH, adsorption time, ion initial concentration). Once the adsorption experiment completed the solution was filtered and the concentration of metal ions in the filtrate was measured by ICP-MS [100]. The adsorption capacity of the polymer toward metal ions (q_e) in mg g^{-1} can be determined by Equation 1:

$$q_e = \frac{(C_o - C_f)V}{W} \qquad (1)$$

where C_o and C_f are initial and final concentration of Lead (II) ions in mg L^{-1}, respectively, W is the weight of the dried terpolymer in g, and V is the volume of solution in L.

2.3 Results and discussion

2.3.1 Synthesis and characterization of TRI and CNT TRI series

The polycondensation reaction between benzene-1,3,5-triamine with paraformaldehyde and alkyldiamine leads to the formation of a cross-linked polyamine (***TRI***) with a high amount of active sites for the removal of lead (II) ions from aqueous solutions. In order to further enhance the adsorption capabilities of the polymers, acylchloride modified carbon nanotubes have been added to the polycondensation reaction and reacted to form a new series of polyamine/CNT composite (***CNT TRI***) for the removal of lead ions from aqueous solutions (figure 2.1).

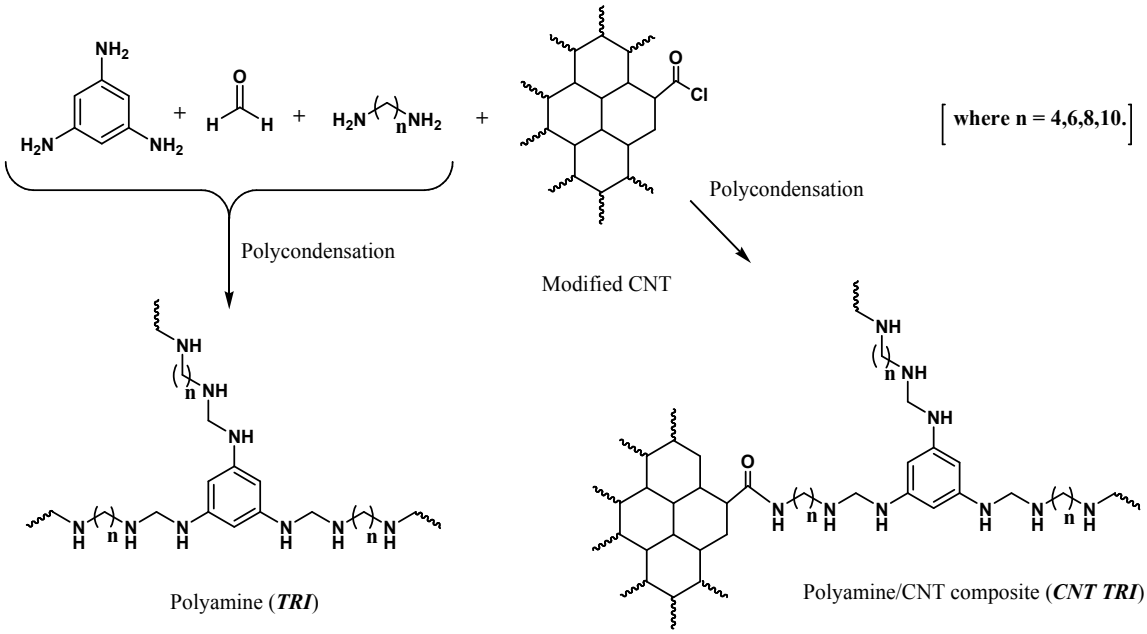

Scheme 2.1 Synthesis of *TRI* and *CNT TRI* series

The synthesized polymers and polymer/CNT composites were characterized by different techniques. The first technique used was FT-IR shown in figure 2.1, similar peaks were found between the polymers in the ***TRI*** series and also in the ***CNT TRI*** series, to show and identify the differences between the ***TRI*** and ***CNT TRI*** series the IR spectra of ***TRI 1,4***, CNT and ***CNT TRI 1,4*** are shown in Figure 2.1. The FT-IR bands identify the structure of the polyamine and the presence of CNT in the structure of composites as follow: A band at ~ 3450 cm^{-1} and a shoulder at ~3270 cm^{-1} attributed for the –NH- and $–NH_2$ stretching vibrations; two bands at ~ 2920 cm^{-1} and 2850 cm^{-1} attributed for the –CH and $–CH_2$ symmetric and asymmetric vibrations; a band at ~ 1640 cm^{-1} attributed for –NH bending vibrations that adds a shoulder at 1585 cm^{-1} in the ***CNT TRI*** series attributed to CNT ncrease in accompanied with a band ~ 1320 cm^{-1} [97]. In addition, the ithe intensity of the band at ~ 1640 cm^{-1} compared to the ***TRI*** series could be attributed to the amide linkage (-C(=O)-NH-) formed between the CNT and the diamines.

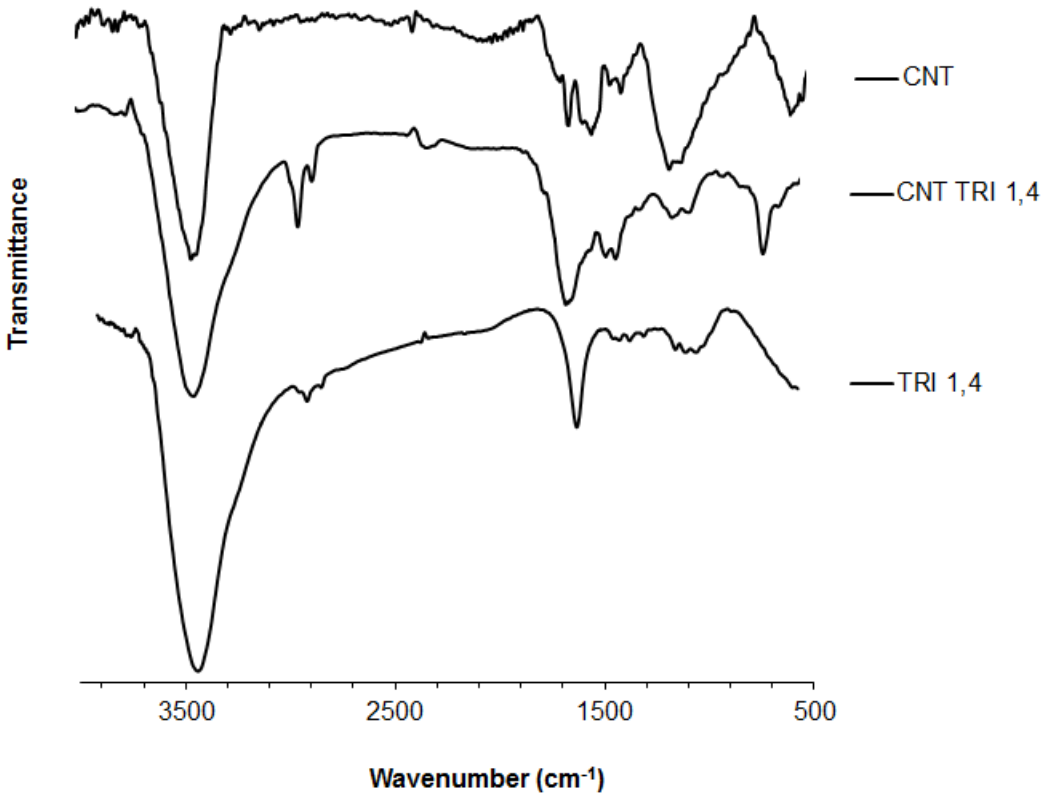

Figure 2.1 FT-IR spectra of the *TRI 1,4,* CNT and *CNT TRI 1,4*.

Figure 2.2 reveals the thermogravimetric analysis of the ***TRI*** and ***CNT TRI*** series. The thermogravimetric analysis of the ***TRI*** series Figure 2.2 (a) and (b) two major decomposition steps; the first ~300ºC which may be attributed to the aliphatic diamine chains followed at ~500ºC the decomposition with aromatic moieties of the benzene-1,3,5-triamine. Whereas the ***CNT TRI*** series is shown in Figure 2.2 (c) and (d) three major decomposition patterns; first at ~ 300ºC the decomposition of the aliphatic diamine moieties followed at ~500ºC the aromatic moieties of the benzene-1,3,5-triamine followed by the decomposition of the CNT at ~600ºC which proves the presence of the CNT in the cross-linked polyamine composite.

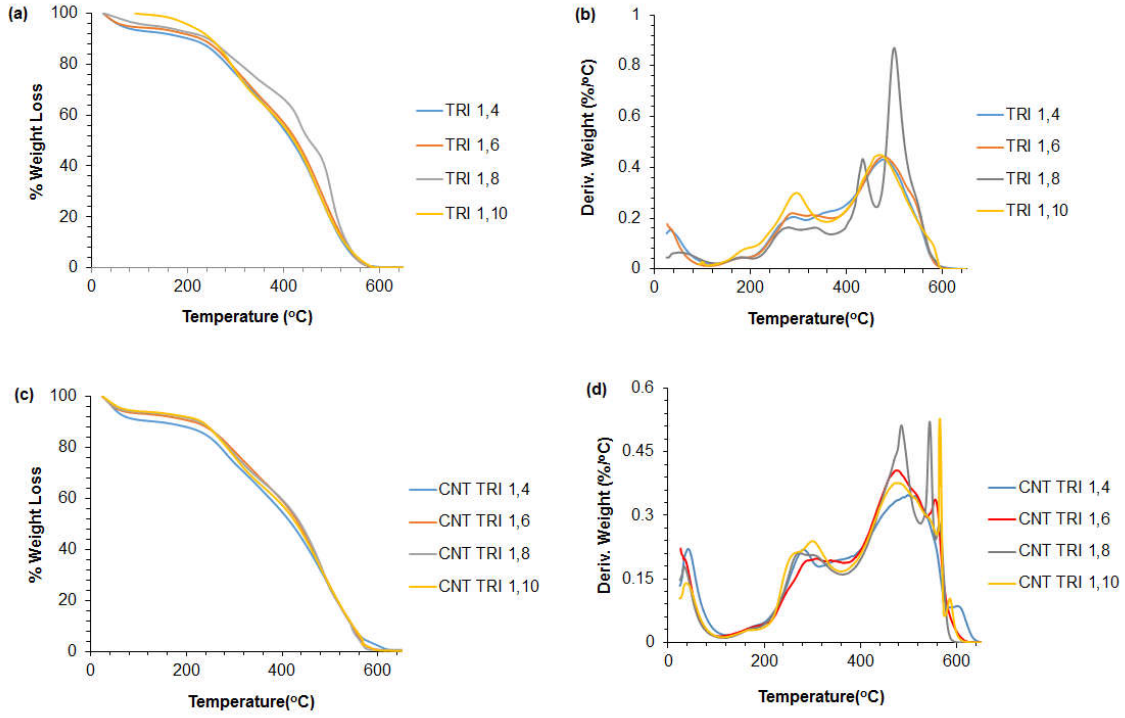

Figure 2.2 (a) Thermogravimetric analysis of the *TRI* series; (b) First derivative of the thermogravimetric analysis of the *TRI* series; (c) Thermogravimetric analysis of the *CNT TRI* series; (d) First derivative of the thermogravimetric analysis of the *CNT TRI* series.

Figure 2.3 reveals the powder X-ray diffraction of the ***TRI*** series, where the cross-linked polyamines are amorphous in nature with the crystallinity increases with the increase of the aliphatic diamine chain from 1,4-diaminobutane to 1,10-diaminodecane which could be attributed better packing in the cross-linked structure. Figure 2.3 also reveals the powder X-ray diffraction of the ***CNT TRI*** series, and as shown in the figure the powder X-ray diffraction shows two peaks one for the amorphous polymer structure at ~2Θ = 20 degrees and a sharp peak at ~2Θ = 25 degree which is distinctive for CNT as reported in the literature [100] and also fits the XRD pattern for CNT. Also, the figure shows a decrease in the intensity of the diffraction peak at ~20 degrees of the ***CNT TRI*** series could be attributed to disordering the arrangements and packing of the cross-linked polyamines

indicating that the synthesis was successful for embedding of the CNT in the ***CNT TRI*** series.

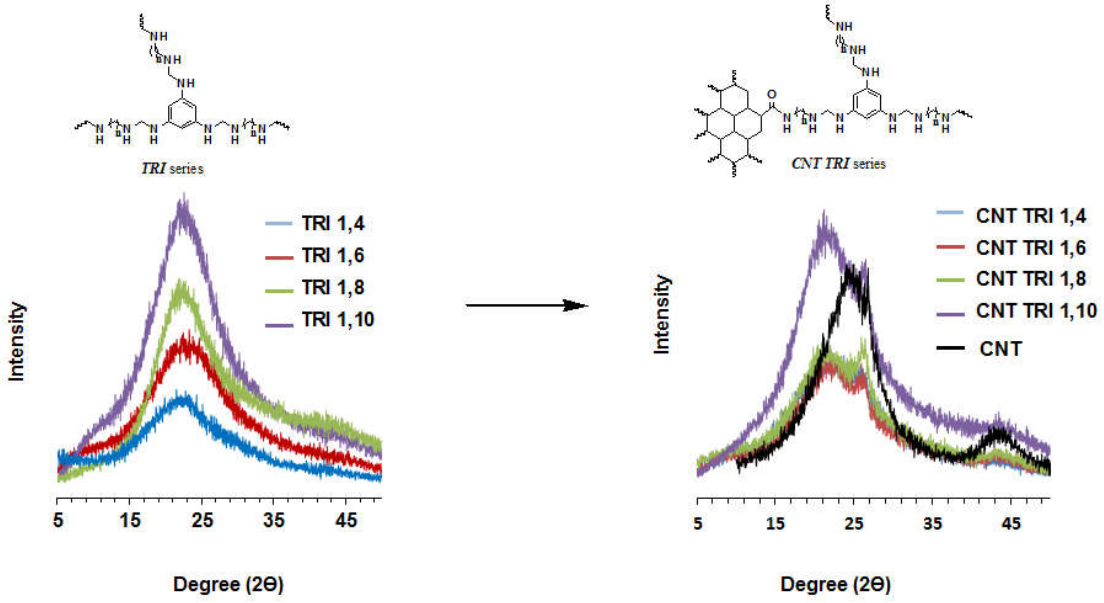

Figure 2.3 Powder x-ray diffraction pattern of the *TRI* and *CNT TRI* series.

2.3.2 Adsorption properties

The adsorption properties of the two series; polyamine (***TRI series***) and polyamine/CNT composite (***CNT TRI*** series) were evaluated for their efficiency to remove lead ions under optimum conditions; where 30 mg of polymer or polymer/CNT composite were added to a 20 ml solution of 5 ppm lead ion prepared using deionized water at pH 6 and stirred for 3 hours at room temperature. The results shown in Figure 2.4, reveal two important factors that affect the adsorption properties of the synthesized materials. First; the effect of alkyldiamine chain length where the adsorption of lead (II) ions decreases with the increase of chain length, which could be explained by the decrease in the attractive amine/repulsive hydrophobic aliphatic methylene chain ratio. The second important factor which can be

seen by enhanced adsorption properties of the polyamine /CNT composites over the polyamines, this could be due to the extra amount of active sites introduced by the addition of CNT. The rest of the adsorption studies were continued on ***TRI 1,4*** and ***CNT TRI 1,4*** composite which is considered the most effective in the removal of lead (II) ions from aqueous solution.

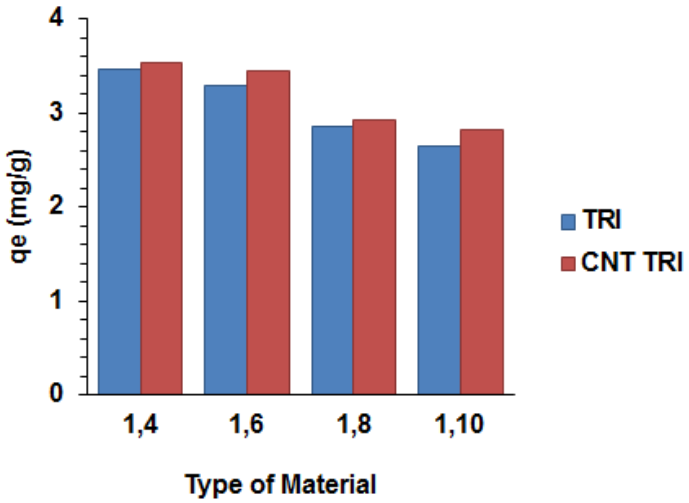

Figure 2.4 The effect of alkyldiamine moiety length on the adsorption of lead (II) ions by both polyamine and polyamine/CNT series

2.3.3 Effect of pH on adsorption of lead by *TRI 1,4* and *CNT TRI 1,4*

The effect was studied by adjusting the pH of the solution by sodium hydroxide (0.1N) and nitric acid (0.1N) solutions. As shown in Figure 2.5; as expected from the presence of the amine moieties in the polyamine and the polyamine/CNT composite the higher pH leads to better adsorption capacity on both ***TRI 1,4*** and ***CNT TRI 1,4*** which is explained by the increased amount of free amines to adsorb lead ions from aqueous solutions [91]. Whereas, at low pH, the protonation of the amine moieties and the formation of the positively charged

ammonium ions leads to the repulsion of lead ions and lower adsorption capacity as shown below:

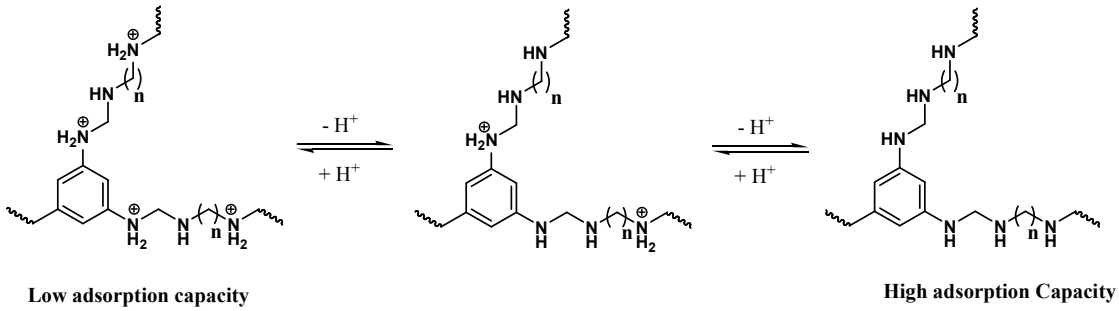

Scheme 2.2 Effect of pH on the protonation of active sites (amine groups)

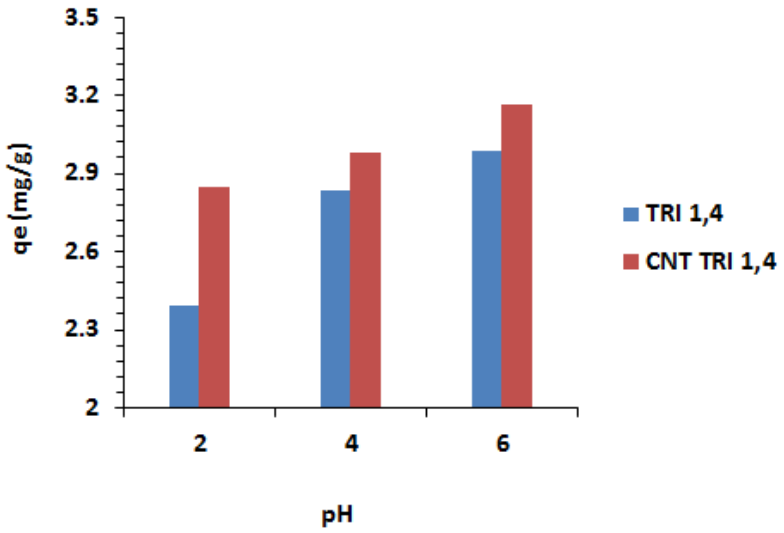

Figure 2.5 The effect of pH on the adsorption capacity of *TRI 1,4* and *CNT TRI 1,4*.

2.3.4 Effect of initial concentration on the adsorption capacity of *TRI 1,4* and *CNT TRI 1,4*

The effect of initial concentration was studied in the range of 1 -5 mg/L, and as shown in the figure 2.6 (a) as the concentration increases the adsorption capacity increases and also

the addition of CNT led to higher adsorption capacity. The experimental data were subjected to three adsorption isotherms, Langmuir, Freundlich and Temkin isotherms [101].

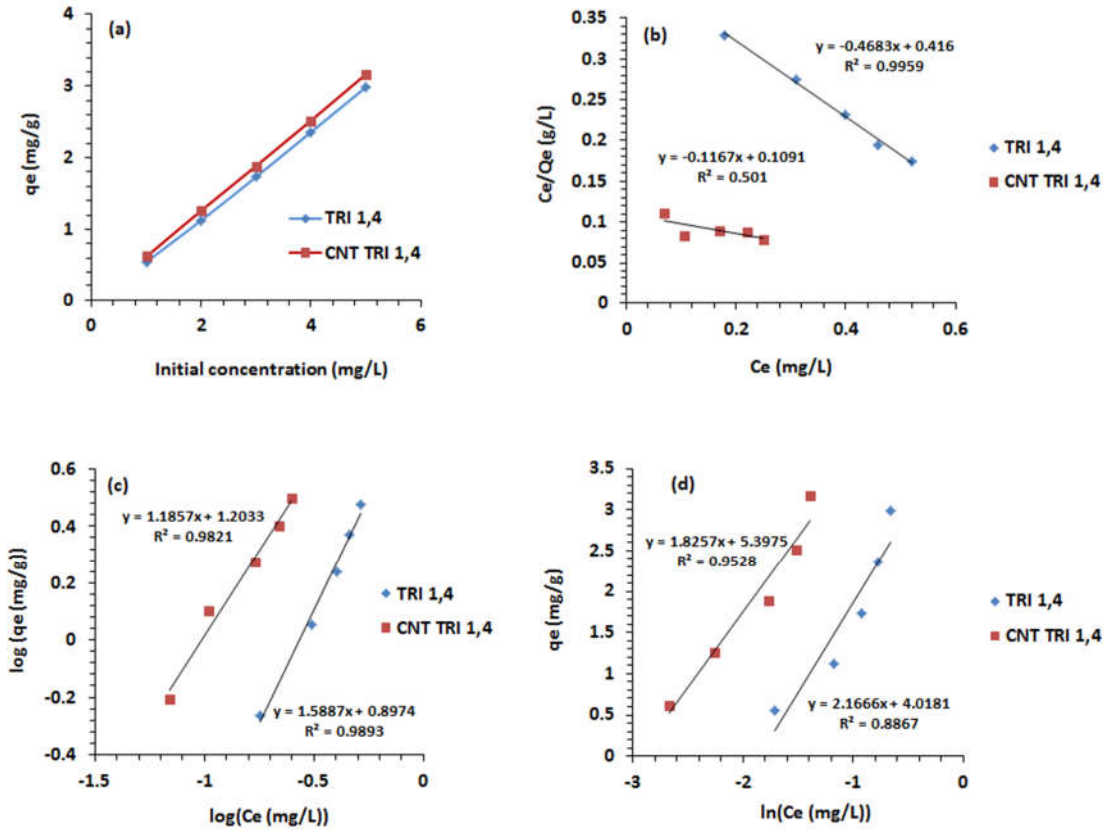

Figure 2.6 (a) Effect of initial concentration on the adsorption capacity of lead ions by *TRI 1,4* and *CNT TRI 1,4*; (b) Langmuir isotherm model; (c) Freundlich isotherm model; (d) Temkin isotherm model

Langmuir adsorption isotherm, which depicts homogeneous adsorption where one lead ion is adsorbed to one active site, can be linearly expressed as follows [102, 103]:

$$\frac{C_e}{q_e} = \frac{C_e}{Q_m} + \frac{1}{bQ_m} \qquad (2)$$

where Qm is the maximum adsorption capacity (mg/g), Ce is the concentration of lead ions left in the solution at equilibrium (mg/L) and ***b*** is the Langmuir constant. As seen from Figure 2.6 (b) and Table 2-2; the experimental data of the ***TRI 1,4*** fit the Langmuir model with a regression value of $R^2 = 0.9959$ while the experimental data of ***CNT TRI 1,4*** do not fit the Langmuir model as indicated by the regression value of $R^2 = 0.5010$. From the data in Table 2-2, the values are calculated and found negative, which assumes that the experimental data of both ***TRI 1,4*** and ***CNT TRI 1,4*** do not fit to the Langmuir model.

Freundlich isotherm model assumes the adsorption to heterogeneous in nature and can be linearly expressed as follows Figure 2.6 (c) [104]:

$$\log q_e = \log k_F + \frac{1}{n} \log C_e \qquad (3)$$

where k_f and $1/n$ are Freundlich isotherm model constant related to adsorption capacity and adsorption intensity. The higher k_f value by ***CNT TRI 1,4*** of 15.97 indicates higher affinity toward lead ions compared to ***TRI 1,4*** with a k_f value of 7.90. The value of $1/n$ if it falls between 0-1 is an indication of chemisorption process and as the value becomes closer to 0 this indicates higher heterogeneity in the surface. As shown in Table 2-2 the value of $1/n$ is closer to zero in the case of ***the TRI 1,4*** compared to ***CNT TRI 1,4***.

The Temkin isotherm model assumes that the energy of the adsorption decreases with the increase in coverage of adsorption sites with lead ions, and can be linearly expressed as follows [105]:

$$q_e = \frac{Rt}{b} lnK_t + \frac{Rt}{b} \ln C_e \qquad (4)$$

where Rt/b (J/mol) and K_T (L/g) are Temkin isotherm constants related to the heat of adsorption and equilibrium binding constant related to the maximum binding energy. *R* is the gas constant (8.314 J/mol. K) and *t* is the temperature (298 K). From the plot and the data in Figure 2.6 (d) and Table 2-2, the experimental data of ***CNT TRI 1,4*** showed better fit to the Temkin isotherm model with a regression value of $R^2 = 0.9528$ compared to ***TRI 1,4*** with a regression value of $R^2 = 0.8867$.

From the isotherm parameters of the three models, it can be concluded that the experimental results fit well with Freundlich isotherm model indicating the favorable heterogeneous nature of the adsorption process.

Table 2-2 Langmuir, Freundlich and Temkin isotherm model constants for the adsorption of lead ions by *TRI 1,4* and *CNT TRI 1,4.*

Metal ion	Material	Langmuir Isotherm Model		
		Qm (mg/g)	*b* (L/mg)	R^2
	TRI 1,4	-2.135	-1.126	0.9959
	CNT TRI 1,4	-8.568	-1.070	0.5010
		Freundlich Isotherm Model		
		k_f	1/*n*	R^2
Pb^{2+}	***TRI 1,4***	7.90	0.63	0.9893
	CNT TRI 1,4	15.97	0.84	0.9821
		Temkin isotherm model		
		b	K_T	R^2
	TRI 1,4	1143	6.39	0.8867
	CNT TRI 1,4	1357	19.2	0.9528

2.3.5 Effect of time on the adsorption of lead ions by TRI 1,4 and CNT TRI 1,4

The effect of time on the adsorption capacity is illustrated in Figure 2.7 (a). From Figure 2.7 (a) the adsorption capacity increases with time, reaching equilibrium within 1 hour for ***CNT TRI 1,4*** whereas for ***TRI 1,4*** the adsorption capacity takes up to 2 hours to reach equilibrium, this could be attributed to the presence of the CNT in ***CNT TRI 1,4***. The experimental data were subjected to two kinetic models; pseudo-second order kinetic model and in order to investigate the adsorption mechanism intraparticle diffusion model was employed.

The pseudo second-order kinetic model developed by Ho in 1995 that describes the adsorption of metal ions to a biomass and assumed that the adsorption may be second-order and the rate determining step may be chemisorption [106]. The linear form of the model can be expressed as follows:

$$\frac{t}{q_t} = \frac{1}{k_2\, q_e^2} + \frac{t}{q_e} \qquad (5)$$

where k_2 is the rate constant in the pseudo second order kinetic model (g/mg. h). q_t represents the adsorption capacity at a certain time (mg/g) and t represents the time (h). From Figure 2.7 (b) and table 2-3; the adsorption process fits the pseudo second-order kinetic model with regression values R^2 ~0.999 assuming that the adsorption process is chemisorption in nature. The second order rate constant (k_2) of ***CNT TRI 1,4*** shows a higher value (8.96) compared to ***TRI 1,4*** (4.00) which implies a higher affinity toward lead ions.

In order to analyze and understand the mechanism of adsorption of lead ions on ***TRI 1,4*** and ***CNT TRI 1,4*** the experimental data were applied to the intraparticle diffusion model which can be linearly expressed as follow [106-108]:

$$qt = k_p t^{0.5} + x \qquad (6)$$

where k_p is rate constant of the intraparticle diffusion model (mg g h^{-1}). x is the intercept which is related to the boundary layer thickness. The intraparticle diffusion model assumes that the adsorption goes through three steps; film diffusion or fast adsorption were lead ions transfers form the bulk of the solution to the surface of the adsorbent, then intraparticle diffusion were lead ions diffuse through the pores of the adsorbent and finally the lead ions are adsorbed on the inner active sites of the adsorbate. In order for the adsorption to be controlled only by intraparticle diffusion the experimental data should pass through the origin of the plot, but sometimes the rate determining step does not pass through the origin and the adsorption process is controlled by film diffusion and intraparticle diffusion. As shown in Figure 2.7 (c), (Table 2-3) the experimental data does not pass through the origin and is controlled by both film diffusion and intraparticle diffusion. The boundary layer thickness x is higher in ***CNT TRI 1,4*** which assumes that the surface diffusion has more influence on the rate determining step compared to ***TRI 1,4***.

Table 2-3 Pseudo second-order and Intraparticle diffusion kinetic model constants for the adsorption of lead ions on *TRI 1,4* and *CNT TRI 1,4*.

Metal ion	Material	Pseudo second-order kinetic model			
		$qe_{(exp)}$ (mg/g)	$qe_{(calc)}$ (mg/g)	k_2	R^2
Pb^{2+}	***TRI 1,4***	2.98	3.05	4.00	0.9999
	CNT TRI 1,4	3.17	3.20	8.96	1.000
		Intraparticle diffusion model			
		x	k_p	R^2	
	TRI 1,4	1.66	1.13	0.9957	
	CNT TRI 1,4	2.65	0.418	0.9902	

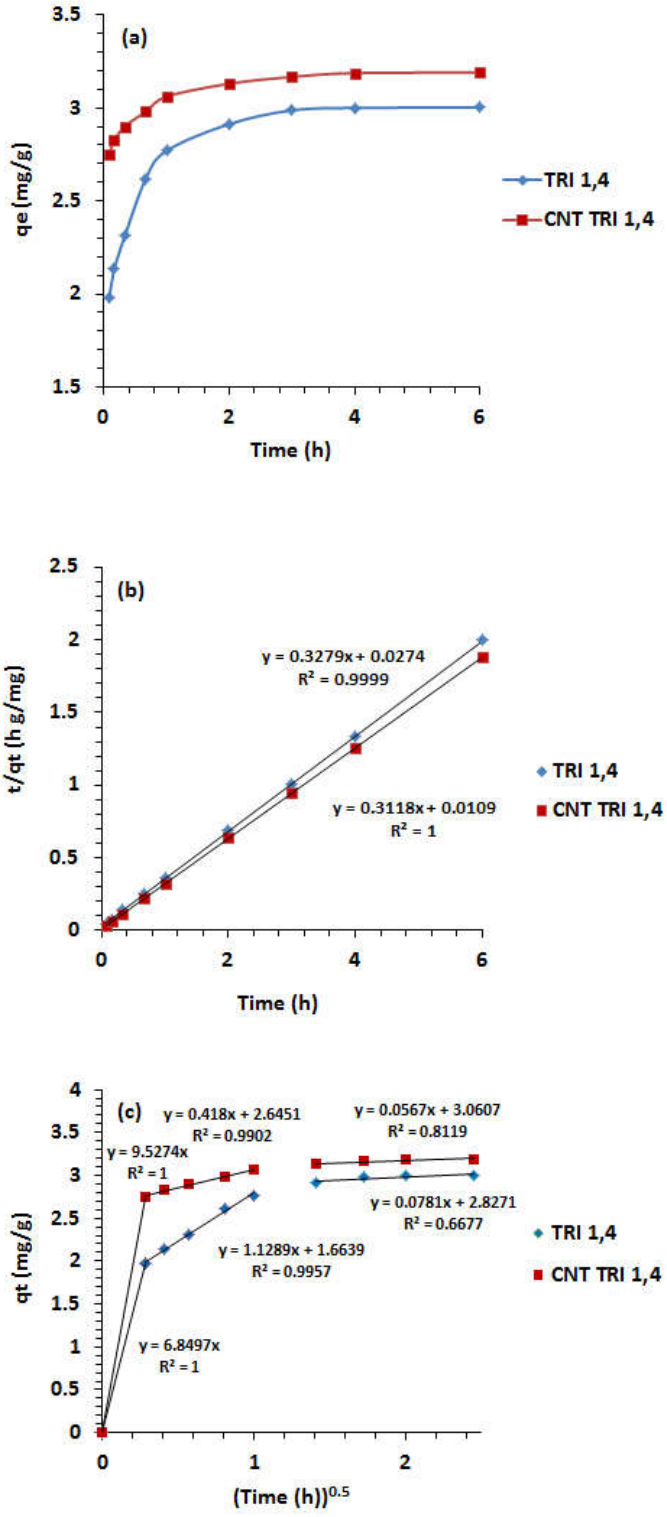

Figure 2.7 (a) effect of time on the adsorption capacity of lead ions by *TRI 1,4* and *CNT TRI 1,4*; (b) Pseudo second-order kinetic model; (c) Intraparticle diffusion model.

2.3.6 Morphology characterization

The morphology of ***TRI 1,4*** and ***CNT TRI 1,4*** was evaluated in order to understand the change that happens after adsorption. The SEM images and EDX spectra of the polymers before and after adsorption were obtained. First, the carbon nanotubes prepared by chemical vapor deposition method were treated with nitric acid to create oxygen containing functional groups. Then, the obtained functionalized nanotubes were treated with thionyl chloride $SOCl_2$, which reacted with the carboxylic groups to produce acylchloride functionalized carbon nanotubes. The defects in the TEM image shown in figure 2.8, indicate, the formation of such sites, however, the tubular structure of carbon nanotube was maintained and preserved. This means the sites were formed on the outer wall of the multiwall carbon nanotubes. These sites work actively as a core from which the polymerization of polyamine may take place.

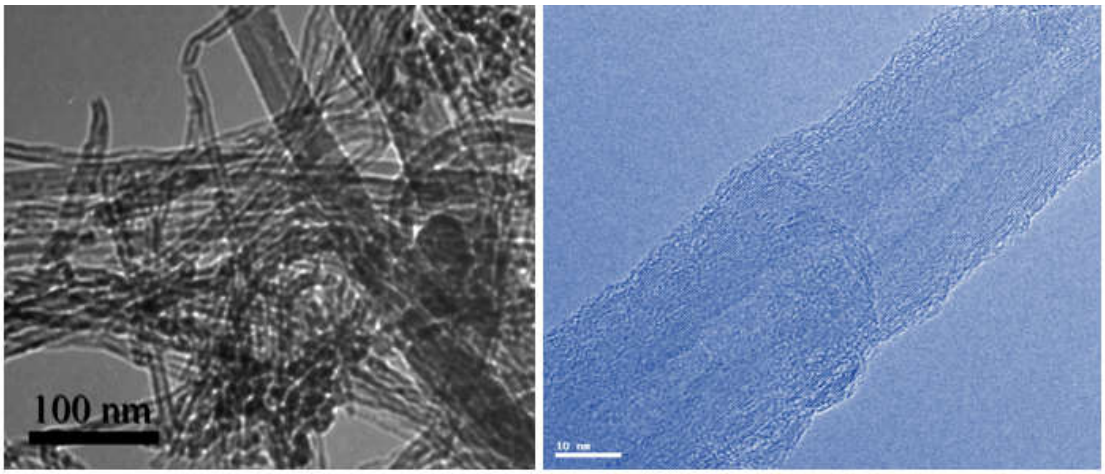

Figure 2.8 TEM images of the CNT used in this study.

The SEM images in Figure 2.9 (a) and (b) indicate there was no notable change in the morphology after adsorption which implies the adsorption may take place via a physical interaction between lead ions and ***TRI 1,4*** polymer. The same can be observed from SEM

images in Figure 2.9 (c) and (d). The EDX spectra of the polymer after adsorption indicate the presence of lead.

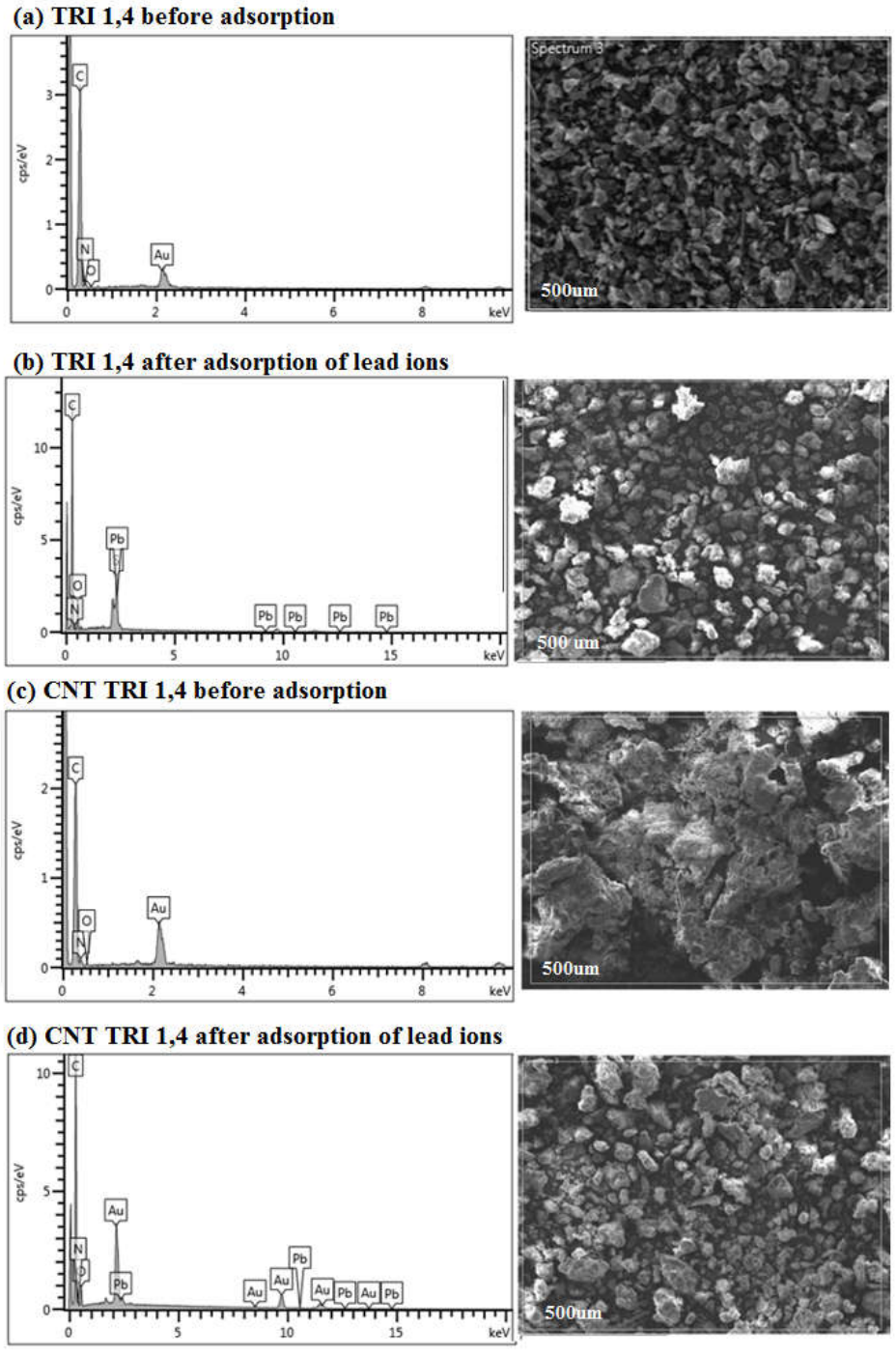

Figure 2.9 (a) SEM and EDX of *TRI 1,4*; (b) *TRI 1,4* loaded with lead ions; (c) SEM and EDX of *CNT TRI 1,4*; (d) *CNT TRI 1,4* loaded with lead ions.

2.4 Conclusion

In our seek for synthesizing novel materials for the removal of toxic metal ions aqueous solutions and to understand the reactions that occur and the mechanism of adsorption, two new series of polymers and polymer CNT composite were synthesized. The cross-linked materials were synthesized in a one pot in-situ polycondensation of benzene-1,3,5-triamine, formaldehyde as a linker and various alkyldiamines to produce the polyamines (***TRI*** series) and with the addition of carbon nanotubes to produce the polyamine/CNT composites (***CNT TRI*** series). The cross-linked polymers and polymer/CNT composites were characterized by different spectroscopic techniques and their structure elucidated. Crystallinity and thermal properties were studied and found that the cross-linked material was amorphous in nature and stable up to ~300^{o}C. Lead ions were chosen as a model toxic metal ion for studying the removal capabilities of the synthesized materials and the adsorption properties were studied under different controlled conditions (pH, time and initial metal concentration). The experimental data fitted Freundlich isotherm model as the adsorption process to be heterogeneous in nature. Also, the adsorption mechanism was studied by applying the kinetic experimental data to an intra-particle diffusion model and found that the adsorption mechanism goes through three steps film diffusion, intra-particle diffusion and then equilibrium. The previous study showed promising results for the synthesis and characterization of new adsorbents for the removal of lead ions from aqueous solution and possible use for treatment of industrial wastewater.

CHAPTER 3

Removal of CO_2 and H_2S by a Sulfur Containing Cross-Linked Porous Polymer for Natural Gas Upgrading

3.1 Introduction

Carbon dioxide (CO_2) and hydrogen sulfide (H_2S) are the primary contaminants in natural gas, the removal of these contaminants is critical for purifying natural gas, because they are corrosive and decrease the heat value [109,110]. Developing new efficient methods for CO_2 and H_2S removal has become promising potential research target for purification of natural gas. A side benefit is to reduce the emission of these gases to the atmosphere [111,112]. Carbon dioxide emissions are the primary source of greenhouse gases; which cause global warming. While hydrogen sulfide, is a corrosive and highly toxic gas for living that can cause severe health issues to including death, in addition to its hazards, it is also known as a corrosive gas [113]. Although the most common conventional method is the liquid chemical scrubbing for these acid gases using amines, this technology has many drawbacks related to low efficiency, high energy consumption, and loss of solvent. Therefore the separation of CO_2 and H_2S gases using porous sorbents with the high internal surface area is a potential alternative due to its high sorption capacity, selectivity, effective cost and efficient energy consumption [114].

The most common studied adsorbents for H_2S removal are shortlisted to metal oxides, metals, metal organic frameworks, MOF's, zeolites, and activated carbon. Massive attention was paid to develop new solid, efficient sorbents with high adsorption capacity and selectivity for CO_2 and H_2S [115], however only limited studies have been done on polymeric materials that are specific for H_2S removal, the most common studied ones where based on amines [116]. The challenges of synthesizing a new polymer for the application of H_2S removal are creating a high surface area to achieve high adsorption capacity, having high selectivity toward H_2S, chemically stable, being regenerable and cost effective [117]. In this study, we characterized a new synthetic porous polymer that efficiently removed H_2S and CO_2 from a mixture of methane (CH_4) mixture similar to the composition of natural gas.

3.2 Materials and Equipment

Pyrrole (98% purity), Paraformaldehyde (≥99% purity) methanol (99.9% purity), hydrochloric acid (37% *w*/*w*) and *N,N*-dimethylformamide (DMF) (99% purity), were obtained from Sigma Aldrich Co. thiophenol (99% purity) was purchased from Fluka. Ammonium hydroxide (25% *w*/*w*) was purchased BDH Limited (Poole, England). Pyrrole and thiophenol were distilled under nitrogen flow at 130 °C and 160 °C respectively, then both were stored under nitrogen environment at 0 °C till it was used. During gas capture experiments, the grade of the used gases were ultra high pure gases were obtained from AHG Industrial Co. (Dammam, Saudi Arabia), CO_2 (99.9%), nitrogen (99.999%), and helium (99.999%).

^{13}C solid-state nuclear magnetic resonance (NMR) spectroscopy measurements were performed on a Bruker 400 MHz spectrometer operating at 125.65 MHz (11.74 T) and ambient temperature (298 K). Samples were packed into 4 mm zirconium oxide (ZrO_2) rotors, and cross-polarization magic angle spinning (CP-MAS) was employed with a pulse delay of 5.0 s and a magic angle spinning rate of 14 kHz. Fourier transform infrared (FT-IR) spectroscopy measurements were performed from KBr pellets using a PerkinElmer 16 PC spectrometer. The spectra were recorded over 4000 – 600 cm-1 in transmission mode and the output signals were described as follows: s, strong; m, medium; w, weak; and by, broad. Thermal gravimetric analysis (TGA) was done on a TA Q-500 instrument with a platinum pan sample holder under air flow with a 10 °C per min heating rate. Powder X-ray diffraction (PXRD) measurements were carried out using a Rigaku MiniFlex II X-ray diffractometer with Cu Kα radiation (λ = 1.54178 Å). Field emission scanning electron microscope (FE-SEM) images were taken on a Tescan LYRA3 Dual Beam microscope at an acceleration voltage of 10 kV. Low-pressure nitrogen sorption isotherms were collected on a Micromeritics ASAP 2020. A liquid nitrogen bath was used for the measurements at 77 K. CO_2, CH_4, and N_2 sorption isotherms were carried out on an Autosorb iQ2 volumetric gas adsorption analyzer. The measurement temperatures at 273 and 298 K were controlled with a water circulator.

3.3 Polymer Synthesis *(THIO-PY)*

In a typical procedure; *p*-formaldehyde (1.80 g, 60 mmol) was mixed with 50 ml DMF in a 100 ml round bottom flask and stirred at room temperature for 10 min [118]. Pyrrole (2.01 g, 30 mmol) was added dropwise followed by thiophenol (1.10 g, 10 mmol) were

added to the reaction flask, stirred for 10 min. moreover, 0.6 ml conc. HCl (12M) was added, and the reaction flask was purged with an N_2 gas and sealed. The reaction was consequently heated under continuous stirring in an oil bath to 363 K for 24 hours. Upon completion of the reaction time, a black solid was filtered and washed with methanol, deionized water, ammonium hydroxide, deionized water and finally thoroughly washed with methanol till a clear filtrate solution was obtained and dried under vacuum at 333 K till constant weight was achieved (3.46 g, yield: 70 % based on monomer weights)). Elemental analysis Calculated (%) for $C_{24}H_{27}N_3S$: C, 74.00; H, 6.99; N, 10.79; S, 8.23. Found: C, 34.53; H, 4.16; N, 8.29; S, 1.65. FT-IR (KBr, 4000 – 500 cm^{-1}): 3442 (br), 2921 (w), 2512 (w), 1637(m), 1405 (w), 1305 (w), 1124 (m), 1037 (m).

3.4 Breakthrough Experimental Measurements

A fixed adsorbent stainless steel column 4 mm inner diameter, 6 mm outer diameter and 20 cm length was filled with the ***THIO-PY*** sample (1.2 g). The column down stream was monitored using a mass spectrometer. The complete setup included check valves, a bypass line (for calibrating the gas concentrations were fed to a mass spectrometer), heater jacket and vacuum pump for regeneration purposes. Testing of wet gas streams (91 % relative humidity. RH), was performed by passing the gas mixture through water vapor saturator (humidifier) at 25 °C until saturation was obtained as detected by mass spectrometry.

The H_2S adsorption tests were performed at room temperature by packing the novel polymers into columns with an inner diameter of ≈2 mm and a length of 200 mm. The quartz was used in both column-ends to maintain the polymer inside the column. The gas containing 2% H_2S was passed through the column of adsorbent at 10 mL/min. The outlet H_2S was monitored using gas chromatography (detector). The excess gas bubbled through

NaOH solution to scrub the toxic acidic H_2S gas for safety reason. The regeneration was performed using nitrogen gas which was flowed through the spent polymer at 60 °C.

3.5 Results and Discussion

A sulfur-containing porous polymer was synthesized by the polycondensation reaction of thiophenol, pyrrole, and *p*-formaldehyde as a linker (Scheme 3.1). The new polymer was permanently porous and revealed potential in the removal of CO_2 and H_2S gases.

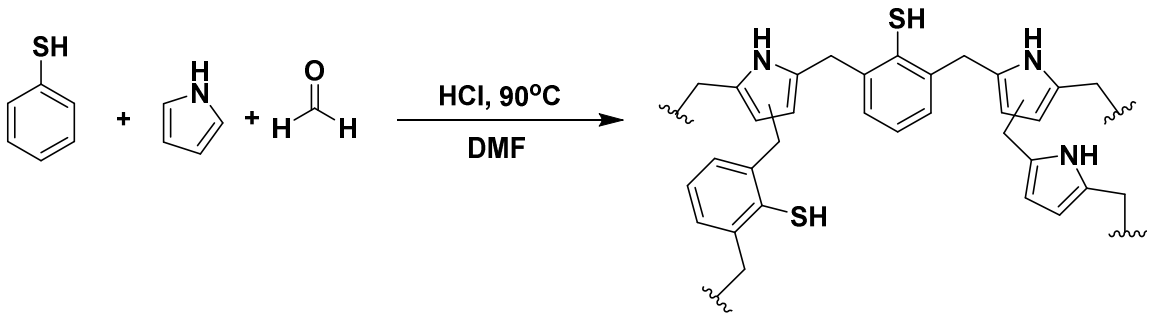

Scheme 3.1. ***THIO-PY*** porous organic polymer synthesis scheme.

The elemental analysis of ***THIO-PY*** showed significant deviation from the calculated theoritical values, which maybe due to incomplete combustion and the presence of trapped gas molecules and water vapors [119, 120]. The FT-IR spectrum shown in Figure 3.1 for ***THIO-PY*** showed a strong, broadband at ~3442 cm^{-1} attributed to the –NH-stretching vibration with the overlap with the –OH stretching found in trapped water molecules. A weak band at ~2921 cm^{-1} attributed to the stretching vibration of the C-H and $–CH_2$-methylene linkages that are absent in thiophenol and pyrrole monomers. A medium band at ~1637 cm^{-1} attributed to the –C=C- aromatic stretching vibration mode found in thiophenol and pyrrole units, a peak at ~1435 cm^{-1} attributed to the –C-N-C- stretching

vibration in the pyrrole moiety. [118, 121]. A weak band at ~2512 cm^{-1} which is almost not seen could be attributed to the –SH stretching vibration found in thiophenol [122].

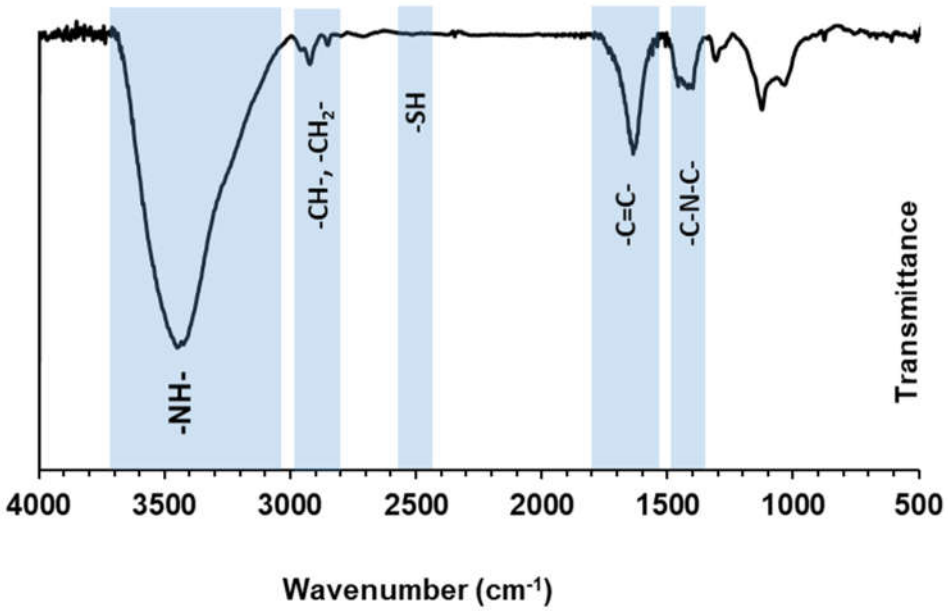

Figure 3.1 FT-IR spectrum for the *THIO-PY* porous organic polymer.

The ^{13}C NMR spectra of ***THIO-PY*** is shown and assigned in figure 3.2. The spectrum revealed a broad peak at ~ 129 ppm which is attributed to the aromatic C atoms found in thiophenol. A shoulder peak at ~140 ppm attributed to the αC linked directly to the nitrogen in the pyrrole moiety. A peak at ~110 ppm attributed to the βC in the pyrrole moiety; and a shoulder peak ~120 ppm attributed to the αC not connected to the methylene between pyrrole and thiophenol. A peak at ~25 ppm is attributed the C atom found in the methylene bridge between the thiophenol and pyrrole moieties [123]. The spectrum agrees with the proposed structure confirming the formation of the proposed polymer [121].

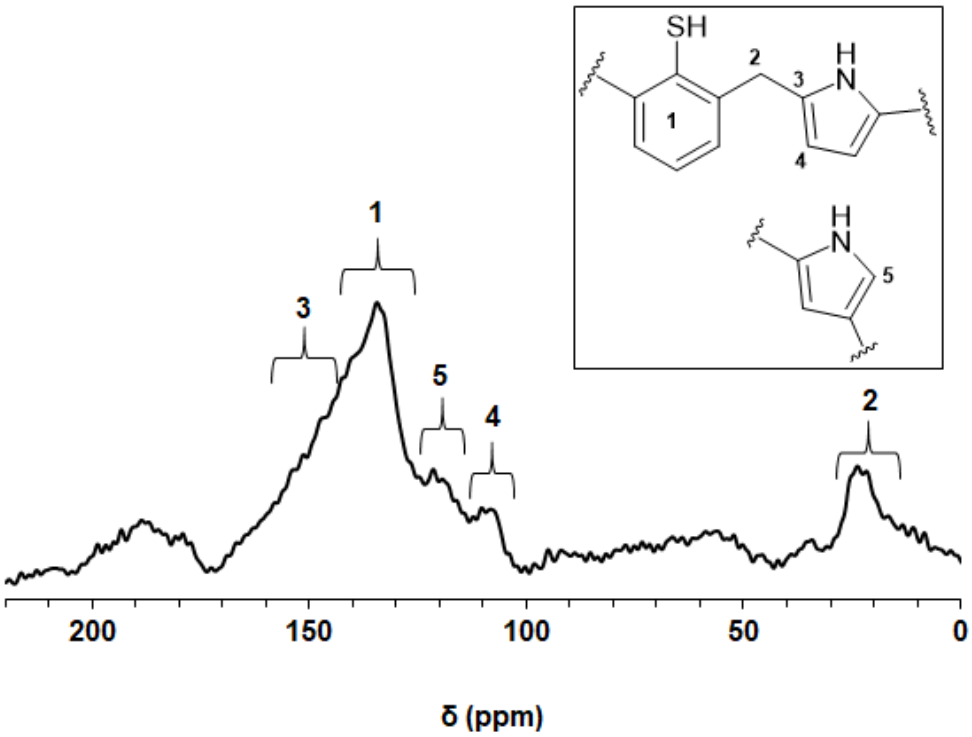

Figure 3.2 CP-CMAS ^{13}C NMR spectrum of the *THIO-PY* polymer.

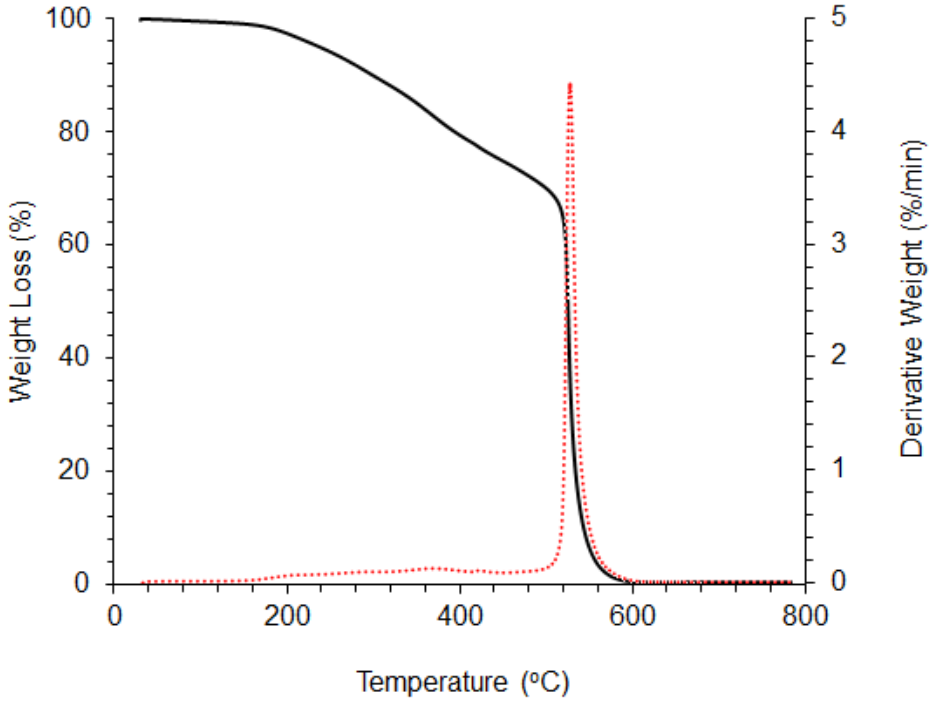

Figure 3.3 Thermogravimetric analysis of *THIO-PY* and its first derivative.

Thermogravimetric analysis of ***THIO-PY*** under air is shown in Figure 3.3 The thermogram and its first derivative reveal that the polymer is stable up to 200ºC above that temperature volatile impurities trapped in the polymeric network are released; This is consistent with deviation observed to the elemental analysis, we attribute this to rearrangement of the polymeric chains to the most stable conformation. At ~545 ºC the thermogram reveals the decomposition point of the polymer. The results show that the polymer is thermally stable and has a great potential to be utilized for industrial applications.

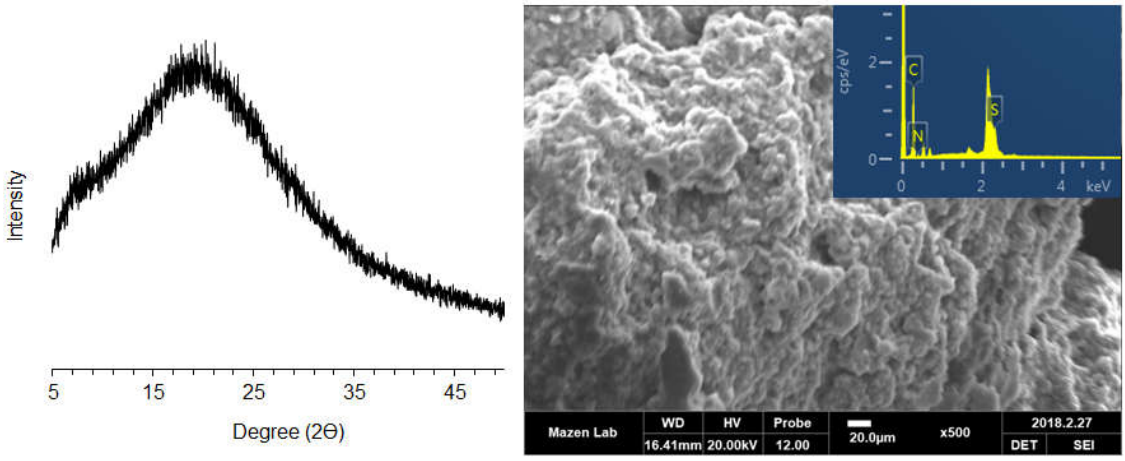

Figure 3.4 Powder X-ray diffraction and SEM-EDX analysis of *THIO-PY*

The morphology and crystallinity of ***THIO-PY*** were analyzed by PXRD and SEM-EDX as shown in Figure 3.4 the PXRD pattern reveals a broad peak ~20 2Θ, which indicates the amorphous nature of the polymer. The SEM image reveals that ***THIO-PY*** has a spherical particle structure and these particles are agglomerated to each other in an amorphous structure which coincides with the PXRD pattern, and that could explain the deviation presence in the elemental analysis; where entrapment of gaseous and water adsorbate molecules within the polymeric structure could explain this deviation. The EDX graph reveals the presence of all the elements proposed in the polymeric structure.

3.5.1 Porosity and textural properties

The permanent porosity of ***THIO-PY*** was evaluated by the adsorption/desorption N_2 isotherm at 77K. Figure 3.5 (a) reveals that *THIO-PY* adopts Type IV isotherm with micro- and mesopores with a BET surface area of 346 $m^2 g^{-1}$ [124]. The N_2 isotherm reveals a rapid uptake at very low relative pressure ($P/P_o < 0.05$) due to the presence of micropores, followed by an incremental increase in the N_2 uptake due to the presence of mesopores ($P/P_o > 0.05$). The hysteresis observed in the desorption isotherm is mainly due to the powder nature of the ***THIO-PY*** polymer [125]. The micro- and mesopores are further confirmed by the QSDFT calculation of pore size distribution shown in figure 3.5 (b) The calculation reveals microporous pore size distribution at below 20 A^o and mesoporous pore size distribution shown as multiple broad peaks below 50 A^o.[126]

3.5.2 Low pressure CO2, CH_4 and N_2 uptake by *THIO-PY*

Due to the permanent porosity and functional nature of the polymer loaded with amine and sulfur groups (-NH- and -SH) that have a high affinity toward CO_2, adsorption/desorption experiments were constructed to evaluate the efficiency of THIO-PY on gas purification and shown in figure 3.5 (c) The uptake values of CO_2 at 273 K and 298 K are 34 and 20 cc/g, respectively. From the adsorption isotherms, the isosteric heat of adsorption of CO_2 was calculated by virial calculation and found to be 32 kJ mol^{-1} for CO_2 Figure 3.5 (d). The CO_2 Q_{st} value with the complete reversible uptake is considered to be preferable for CO_2 capture from flue gas as reported by Wilmer et al. [127] the high Q_{st} value toward CO_2 is correlated with the high concentration of nitrogen groups allocated in ***THIO-PY*** [128]. the Q_{st} value for CH_4 was calculated by the virial method and found to be 18 kJ mol^{-1} which is considered to be high but is comparable to functionalized organic porous polymers [129].

as noted in Figure 3.5 (d) the Q_{st} value increases with the increase in coverage, and that could be explained by cooperative interactions between CH_4 molecules leading to the increase in the Q_{st} value [130].

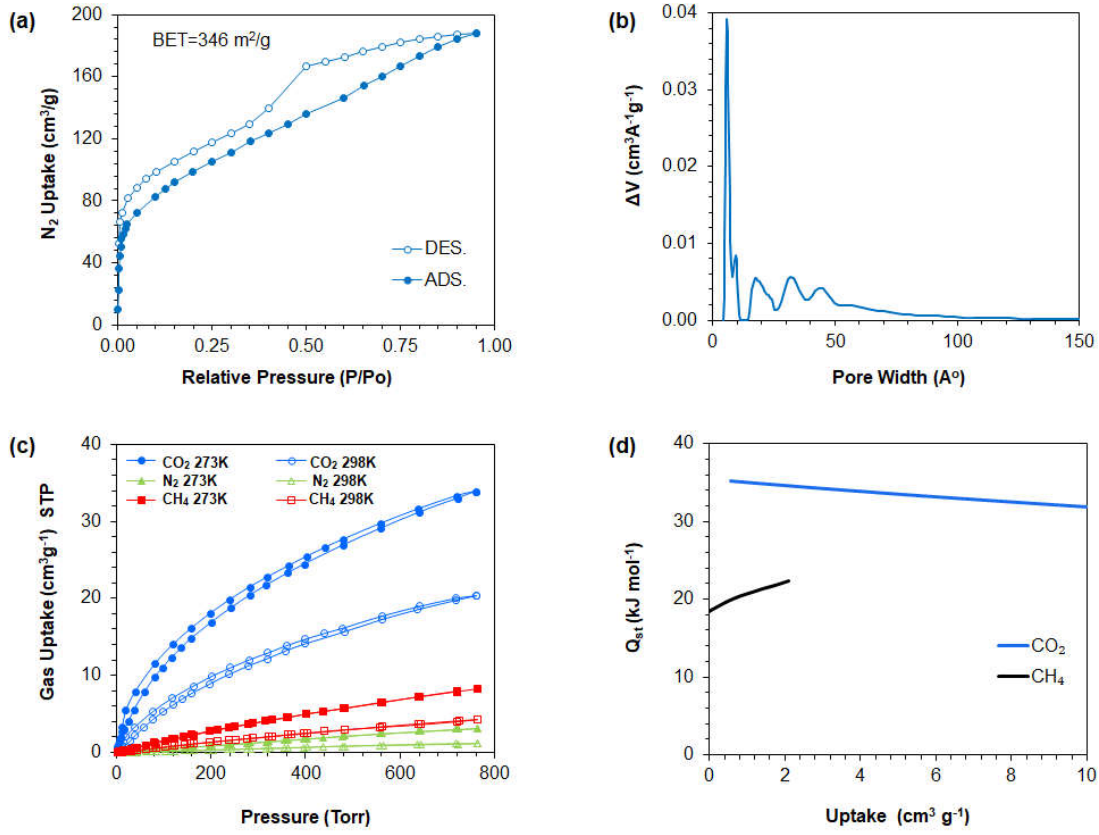

Figure 3.5 (a) N_2 adsorption/desorption isotherm of *THIO-PY* at 273K; (b) DFT pore size distribution of *THIO-PY*;(c) CO_2 and N_2 adsorption isotherms at 273K and 298K of *THIO-PY*; (d) *THIO-PY* isosteric heats of absorption for CO_2 and CH_4.

3.5.3 Breakthrough experiments of CO_2 and H_2S

In order to evaluate the efficiency and selectivity of THIO-PY polymer toward the capture of CO_2, an activated sample was exposed to a stream of a gaseous mixture of 10% (*v*/*v*) CO_2 and 90% (*v*/*v*) CH_4. The effluent gas was monitored for the breakpoint in the breakthrough time by an online mass spectrometer (which is calculated based on the

breakpoint when the concentration of CO_2 exiting the bed is equal to 5% the original concentration). The first experiment shown in Figure 3.6 (a), reveals that the dynamic uptake capacity of 8.9 cc g^{-1} in dry conditions. The uptake capacity almost doubled in the wet breakthrough experiment without the loss in activity with an average of 18.3 cc g^{-1}. The results indicate the high potential of ***THIO-PY*** to be utilized for the separation of CO_2 from natural gas streams.

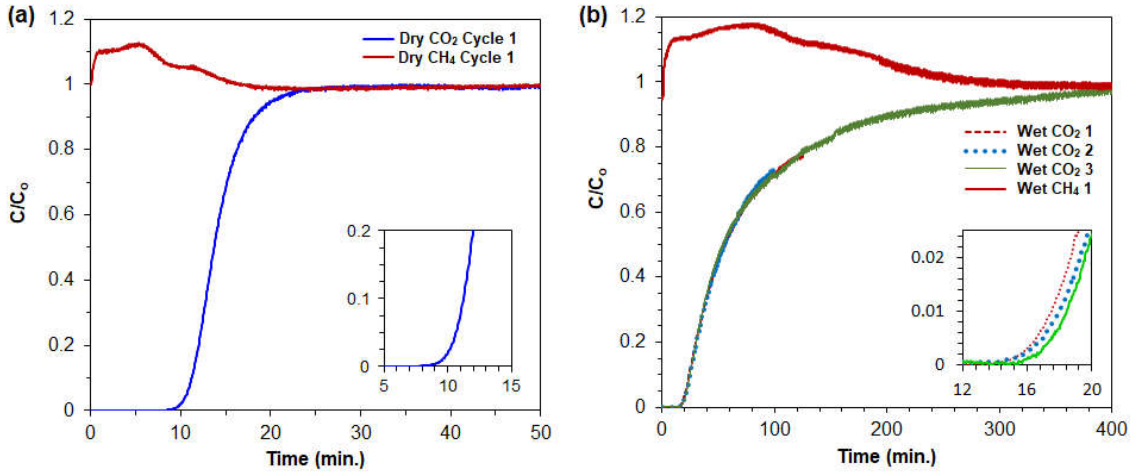

Figure 3.6 *THIO-PY* **Breakthrough results of (Adsorbent mass = 1.2 g, T=298 K, P= 1 bar (ambient conditions) inlet gas mixture = 10 sccm of CO_2 and CH_4 mixture (0.1 and 0.9 molar fraction) (a) Dry CO_2 breakthrough; (b) Wet CO_2 breakthrough (Relative humidity = 91%). Note: breakthrough capacity breakpoint was evaluated based on 5% of the original CO_2 concentration)**

Encouraged by the results obtained by the breakthrough experiments for CO_2 separation. We considered the presence of H_2S in the natural gas stream. H_2S is considered one of the major concerns in the natural gas industry, due to its corrosiveness nature, toxicity and flammability [112]. The presence of CO_2 in the natural gas stream with higher concentration and higher acidity than H_2S limits the removal of H_2S and causes several difficulties even with the already used major techniques such as the Claus process where incomplete conversion of H_2S due to high temperatures used in the process [112, 131, 132].

In order to test the performance and stability of ***THIO-PY*** polymer, a 2% H_2S in methane gas mixture was passed through a column that contained 0.5 g of ***THIO-PY***, the results in figure 3.7 reveal a breakthrough point (5% of the original concentration) at around 160 min. Which is equivalent to an adsorption capacity of 97.1 mg/g, regeneration of THIO-PY was performed by a flow of N_2 gas at 60^{o}C for 1 hour. The amount of H_2S removed by this polymer is considered one of the top performing polymer adsorbents reported in the literature. The high adsorption capacity could be attributed to the presence of amine and thiol groups which could attract H_2S by electrostatic attraction caused by hydrogen bonding between the amine and thiol groups with H_2S [133, 134]. Screening the literature revealed the lack of adsorbents for H_2S removal due to the degradation of the material when in contact with H_2S, low regeneration capability as shown in Table 3-1.

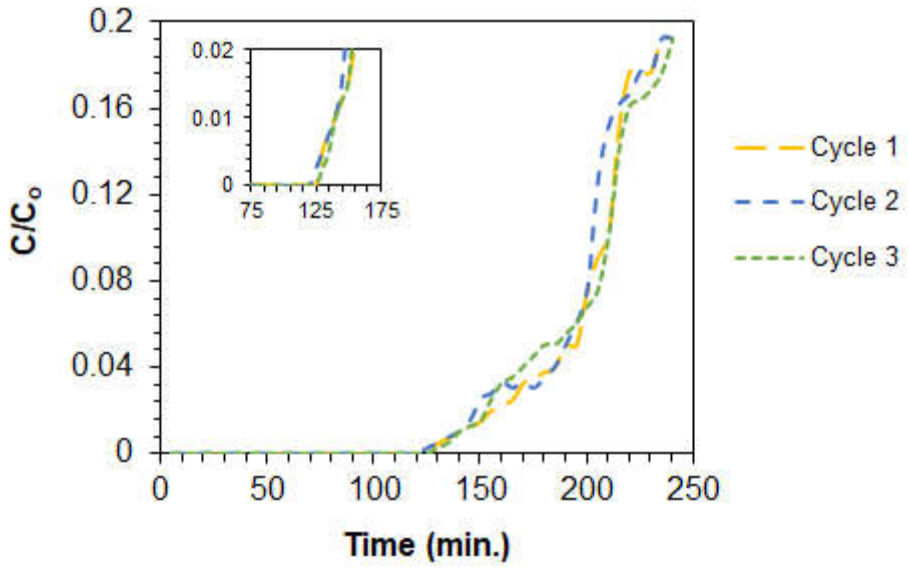

Figure 3.7 *THIO-PY* **breakthrough results for three cycles of 2% H_2S in CH_4 gas mixture**

Material	Surface area (m^2/g)	Adsorption capacity (mg/g)	Regeneration capacity (%)	Regeneration temperature (^oC)	Ref.
Mixed Copper-based metal oxides	16.4 -96.7	17.7 - 114	75	100	[135]
Metal oxide/activated carbon	139 - 641	8 - 110	18-27	400	[136, 137]
Titanosilicates	200	10.8 - 47.6	-	-	[138]
THIO-PY	346	97.1	100%	60	This work

Table 3-1 BET surface area and breakthrough capacity of various materials

3.6 Conclusion

A new efficient polymeric adsorbent has been synthesized via Freidel craft alkylation of thiophenol, pyrrole, and formaldehyde as a cross-linker. Taking into consideration the properties of an efficient adsorbent that has a high affinity toward CO_2 and H_2S gases. Revealed a high potential for the utilization in natural gas upgrading. The resultant ***THIO-PY*** polymer showed permanent porosity with a surface area of 346 m^2/g and excellent adsorption capacity of CO_2 under dry and wet conditions. The results revealed that the adsorption capacity of CO_2 doubled in the presence of humidity. Encouraged by the stability and robustness of ***THIO-PY*** in dry a wet conditions the polymer was further investigated for its capability to remove H_2S. The results revealed that ***THIO-PY*** is among the highest adsorption capacity of 97.1 mg/g and among the most efficient as it is regenerated at low temperatures compared to the literature.

References

1. Ghorbani M, Abbas Abad Arabi J, Izanlou Z, Kazempour Sabahi SH. Nano-Photo catalysts and their application in water and wastewater treatment. The first national conference on new technologies in the chemical and petrochemical 2014.
2. Filipponi L and Sutheraland D. Applications of Nanothechnology: Environment. Nanocap, Nanothechnology Capacity Building NGOs 2007.
3. Krantzberg G, Tanik A, do Carmo J.S.A., Indarto A, Ekda A. Advances in water quality control. Scientific Research Publishing 2010.
4. Yunus I, Harwin, Kurniawan A, Adityawarman D, Indarto A. Nanotechnologies in water and air pollution treatment. Environmental Technology Reviews 2012; 1(1): 136–148.
5. Environmental Defense Fund. The health risks of burning coal for energy. Report 2006. Available at http://www.edf.org/climate/remaking-energy.
6. I. Ali, V.K. Gupta, Advances in water treatment by adsorption technology, Nat. Protoc. 1 (2007) 2661–2667.
7. V.K. Gupta, P.J.M. Carrott, M.M.L. Ribeiro Carrott, Suhas, Low-cost adsorbents: growing approach to wastewater treatment - a review, in: Crit. Rev. Environ. Sci. Technol. 39 (2009) 783–842.
8. M. Alkan, M. Dogan, Adsorption of copper(II) onto perlite, J. Colloid Interface Sci. 243 (2001) 280–291.
9. M. Halim, P. Conte, A. Piccolo, Potential availability of heavy metals to phytoextraction from contaminated soils induced by exogenous humic substances, Chemosphere 52 (2002) 26–75.
10. R. Balasubramanian, S.V. Perumal, K. Vijayaraghavan, Equilibrium isotherm studies for the multicomponent adsorption of lead, zinc, and cadmium onto Indonesian peat, Ind. Eng. Chem. Res. 48 (2009) 2093–2099.
11. V.K. Gupta, I. Ali, Removal of lead and chromium from wastewater using bagasse fly ash – a sugar industry waste, J. Colloid Interface Sci. 271 (2004) 321–328.

12. R.A.K. Rao, M. Kashifuddin, Kinetics and isotherm studies of Cd (II) adsorption from aqueous solution utilizing seeds of bottlebrush plant (Callistemon chisholmii), Appl. Water Sci. 4 (2014) 371–383.
13. Human health and heavy metals exposure, in: H. Howard, M.C. Michael (Eds.), Life Support: The Environment and Human Health, MIT Press, 2002, Chapter 4.
14. Drinking water [FAD 25: Drinking Water], Indian Standard Drinking Waterspecification (Second Revision), ICS 13.060.20 IS 10500, 2012.
15. M. Ahmaruzzaman, Industrial wastes as low-cost potential adsorbents for the treatment of wastewater laden with heavy metals, Adv. Colloid Interface Sci. 116 (2011) 36–59.
16. Deborah F. Shmueli, Water quality in international river basins, Political Geography 18 (1999) 437–476.
17. M.A. Khan, M.K. Uddin, R. Bushra, A. Ahmad, S.A. Nabi, Synthesis and characterization of polyaniline Zr(IV) molybdophosphate for the adsorption of phenol from aqueous solution, React. Kinet. Mech. Catal. 113 (2014) 499– 517.
18. R.A.K. Rao, S. Ikram, M.K. Uddin, Removal of Cr (VI) from aqueous solution on seeds of Artimisia absinthium (novel plant material), Desalin. Water Treat. 54 (2015) 3358–3371.
19. R.A.K. Rao, S. Ikram, M.K. Uddin, Removal of Cd (II) from aqueous solution by exploring the biosorption characteristics of gaozaban (Onosma bracteatum), J. Environ. Chem. Eng. 2 (2014) 1155–1164.
20. R.A.K. Rao, M. Kashifuddin, Adsorption properties of coriander seed powder (Coriandrum sativum): extraction and pre-concentration of Pb (II), Cu (II) and Zn (II) ions from aqueous solution, Adsorpt. Sci. Technol. 30 (2012) 127–146.
21. R.A.K. Rao, F. Rehman, M. Kashifuddin, Removal of Cr (VI) from electroplating wastewater using fruit peel of Leechi (Litchi chinensis), Desalin. Water Treat. 49 (2012) 136–146.
22. V.K. Gupta, R. Kumar, A. Nayak, T.A. Saleh, M.A. Barakat, Adsorptive removal of dyes from aqueous solution onto carbon nanotubes: a review, Adv. Colloid Interface Sci. 193 (2013) 24–34.

23. Shannon, M. A.; Bohn, P. W.; Elimelech, M.; Georgiadis, J. G.; Marinas, B. J.; Mayes, A. M. Science and technology for water purification in the coming decades. Nature 2008, 452 (7185), 301.
24. Bhattacharyya, K. G.; Sen Gupta, S. Adsorption of a few heavy metals on natural and modified kaolinite and montmorillonite: A review. Adv. Colloid Interface Sci. 2008, 140 (2), 114.
25. Kongsricharoern, N.; Polprasert, C. Electrochemical precipitation of chromium (Cr6+) from an electroplating wastewater. Water Sci. Technol. 1995, 31 (9), DOI: 10.1016/0273-1223(95)00412-G.
26. Dialynas, E.; Diamadopoulos, E. Integration of a membrane bioreactor coupled with reverse osmosis for advanced treatment of municipal wastewater. Desalination 2009, 238 (1), 302.
27. Abo-Farha, S. A.; Abdel-Aal, A. Y.; Ashour, I. A.; Garamon, S. E. Removal of some heavy metal cations by synthetic resin purolite C100. J. Hazard. Mater. 2009, 169 (1), 190.
28. Kabdaşlı, I.; Arslan, T.; Ölmez-Hancı, T.; Arslan-Alaton, I.; Tünay, O. Complexing agent and heavy metal removals from metal plating effluent by electrocoagulation with stainless steel electrodes. J. Hazard. Mater. 2009, 165 (1), 838.
29. Bhatnagar, A.; Sillanpaa, M. Utilization of agro-industrial and municipal waste materials as potential adsorbents for water treatmentA review. Chem. Eng. J. 2010, 157 (2-3), 277.
30. Yee, K. K.; Reimer, N.; Liu, J.; Cheng, S. Y.; Yiu, S. M.; Weber, J.; Stock, N.; Xu, Z. T. Effective Mercury Sorption by Thiol-Laced Metal-Organic Frameworks: in Strong Acid and the Vapor Phase. J. Am. Chem. Soc. 2013, 135 (21), 7795.
31. Fu, F.; Wang, Q. Removal of heavy metal ions from wastewaters: A review. J. Environ. Manage. 2011, 92 (3), 407.
32. Yuanyuan Ge and Zhili Li , Application of Lignin and Its Derivatives in Adsorption of Heavy Metal Ions in Water: A Review ACS Sustainable Chem. Eng. 2018, 6, 7181-7192.
33. J.G. Pounds, G.J. Long, J.F. Rosen, Cellular and molecular toxicity of lead in bone, Environ. Health Perspect. 91 (1991) 17–32.

34. P. Gustavsson, L. Gerhardsson, Intoxication from an accidentally ingested lead shot retained in the gastrointestinal tract, Environ. Health Perspect. 113 (2005) 491–493.
35. I. Lancranjan, H.I. Popescu, O. Gavanescu, I. Klepsch, M. Serbanescu, Reproductive ability of workmen occupationally exposed to lead, Arch. Environ. Health 30 (1975) 396–401.
36. W.C. Cooper, O. Wong, L. Kheifets, Mortality among employees of lead battery plants and lead-producing plants, 1947–1980, J. Work Environ. Health 11 (1985) 331–345.
37. L. Gerhardsson, N.G. Lundström, G. Nordberg, S. Wall, Mortality and lead exposure: a retrospective cohort study of Swedish smelter workers, Br. J. Ind. Med. 43 (1986) 707–712.
38. R.L. Canfield, C.R. Henderson, D.A. Cory-Slechta, C. Cox, T.A. Jusko, B.P. Lanphear, Intellectual impairment in children with blood lead concentrations below 10 ug per deciliter, N. Eng. J. Med. 348 (2003) 1517–1526.
39. B.P. Lanphear, T.D. Matte, J. Rogers, R.P. Clickner, B. Dietz, R.L. Bornschein, et al., The contribution of lead-contaminated house dust and residential soil to children's blood lead levels. A pooled analysis of 12 epidemiologic studies, Environ. Res. 79 (1998) 51–68.
40. K.N. Dietrich, M.D. Ris, P.A. Succop, O.G. Berger, R.L. Bornschein, Early exposure to lead and juvenile delinquency, Neurotoxicol. Teratol. 23 (2001) 511–518.
41. Mohammad Kashif Uddin , A review on the adsorption of heavy metals by clay minerals, with special focus on the past decade, Chemical Engineering Journal 308 (2017) 438–462.
42. D.H. Lee, H. Moon, Adsorption equilibrium of heavy metals on natural zeolites, Korean J. Chem. Eng. 18 (2001) 247–256.
43. I.L. Lagadic, M.K. Mitchell, B.D. Payne, Highly effective adsorption of heavy metal ions by a thiol-functionalized magnesium phyllosilicate clay, Environ. Sci. Technol. 35 (2001) 984–990.
44. S.D. Cunningham, J.R. Shann, D.E. Crowley, T.A. Anderson, Phytoremediation of contaminated water and soil, J. Am. Chem. Soc. 1 (1997) 2–17.

45. Muharram Ince, Olcay Ince, An Overview of Adsorption Technique for Heavy Metal Removal from Water/Wastewater: A Critical Review, Int. J. Pure Appl. Sci. 3(2): 10-19 (2017).
46. WHO, 9 out of 10 people worldwide breathe polluted air, but more countries are taking action, <http://www.who.int/news-room/detail/02-05-2018-9-out-of-10-people-worldwide-breathe-polluted-air-but-more-countries-are-taking-action>, 2 May 2018
47. J.T. Houghton, Y. Ding, D.J. Griggs, M. Noguer, P.J. Linden, X. Dai, K. Maskell, C.A. Johnson, Climate Change: The Scientific Basis, Intergovernmental Panel on Climate Change, 2001.
48. Redrawing the Energy-Climate Map, Organisation for Economic Co-operation and Development (OECD)/International Energy Agency (IEA), France, 2013.
49. R.H. Williams, Toward Zero Emissions from Coal in China, China Clean Energy Forum, China, 2001.
50. NASA, Global temperature, https://climate.nasa.gov/.
51. M.Z. Jacobson, of Review solutions to global warming, air pollution, and energy security Energy Environ. Sci. 2 (2009) 148.
52. M. Hoeven, CO2 Emissions from Fuel Combustion Highlights, International Energy Agency, 2013.
53. US EPA, global greenhouse gas emission data, 2010 https://www.epa.gov/ghgemissions/global-greenhouse-gas-emissions-data
54. T.A., Marland, G., and Andres, R.J. National CO2 Emissions from Fossil-Fuel Burning, Cement Manufacture, and Gas Flaring: 1751-2014 http://cdiac.ess-dive.lbl.gov/trends/emis/top2014.tot
55. Kyoto Protocol to the United Nations Framework Convention on Climate Change, United Nations, 1998.
56. T. Dixon, G. Leamon, P. Zakkour, L. Warren, Energy Proceed. 37 (2013) 7596.
57. Ciferno, J.P., Fout, T.E., Jones, A.P., Murphy, J.T., 2009. Capturing carbon existing coal-fired power plants. Chem. Eng. Prog. 105, 33–41
58. D'Alessandro, D.M., Smit, B., Long, J.R., 2010. Carbon dioxide capture: prospects for new materials. Angew. Chem. Int. Ed. 49, 6058–6082

59. Spigarelli, B.P., Kawatra, S.K., 2013. Opportunities and challenges in carbon dioxide capture. J. CO2 Utilization 1, 69–87.
60. Baltrėnaitė, E., Baltrėnas, P., Lietuvninkas, A., 2016. The Sustainable Role of the Tree in Environmental Protection Technologies. Springer International Publishing, Switzerland.
61. Solar, C., García Blanco, A., Vallone, A., Sapag, K., 2010. In: Potocnik, P. (Ed.), Adsorption of methane in porous materials as the basis for the storage of natural gas. Intech, Rijeka, pp. 205–244.
62. Figueroa, J.D., Fout, T., Plasynski, S., McIlvried, H., Srivastava, R.D., 2008. Advances in CO2 capture technology—the U.S. Department of Energy's Carbon Sequestration Program. International Journal of Greenhouse Gas Control 2, 9–20.
63. Songolzadeh, M., Takht Ravanchi, M., Soleimani, M., 2012. Carbon dioxide capture and storage: a general review on adsorbents. Int. J. Chem. Mol. Nucl. Mater. Metall. Eng. 6, 900–907.
64. Cinke, M., Li, J., Bauschlicher Jr., C.W., Ricca, A., Meyyappan, M., 2003. CO2 adsorption in single-walled carbon nanotubes. Chem. Phys. Lett. 376, 761–766.
65. Lu, C., Bai, H., Wu, B., Su, F., Hwang, J.F., 2008. Comparative study of CO2 capture by carbon nanotubes, activated carbons, and zeolites. Energy Fuel 22, 3050–3056
66. Smart, S.K., Cassady, A.I., Lu, G.Q., Martin, D.J., 2006. The biocompatibility of carbon nanotubes. Carbon 44, 1034–1047.
67. Yang, R. T. Adsorbents: Fundamentals and Applications; WileyInterscience: Hoboken, NJ, 2003.
68. Yong, Z.; Mata, V.; Rodrigues, A. E. Adsorption of carbon dioxide at high temperature—A review. Sep. Purifi. Technol. 2002, 26, 195–205.
69. Zheng, F.; Addleman, R. S.; Aardahl, C. L.; Fryxell, G. E.; Brown, D. R.; Zemanian, T. S. Amine functionalized nanoporous materials for carbon dioxide (CO2) capture. Environmental Applications of Nanomaterials: Synthesis, Sorbents and Sensors; Fryxell, G. E., Cao, G., Eds.; Imperial College Press: Singapore, 2007; pp 285311.
70. Sayari, A.; Belmabkhout, Y.; Serna-Guerrero, R. Flue gas treatment via CO2 adsorption. Chem. Eng. J. 2011, 171, 760–774.

71. Gray, M. L.; Champagne, K. J.; Fauth, D.; Baltrus, J. P.; Pennline, H. Performance of immobilized tertiary amine solid sorbents for the capture of carbon dioxide. Int. J. Greenhouse Gas Control 2008, 2, 3–8.
72. Li, Y., Yi, H., Tang, X., Li, F., Yuan, Q., 2013. Adsorption separation of CO2/CH4 gas mix on the commercial zeolites at atmospheric pressure. Chem. Eng. J. 229, 50–56.
73. Arunkumar Samanta, An Zhao, George K. H. Shimizu, Partha Sarkar, and Rajender Gupta Post-Combustion CO2 Capture Using Solid Sorbents: A Review, Ind. Eng. Chem. Res. 2012, 51, 1438–1463.
74. Adams, D. Flue Gas Treatment for CO2 Capture; IEA Clean Coal Centre: London, 2010.
75. Tarka, T. J.; Ciferno, J. P.; Gray, M. L.; Fauth, D. CO2 capture systems using amine enhanced solid sorbents. Presented at the Fifth Annual Conference on Carbon Capture & Sequestration, Alexandria, VA, USA, May 811, 2006; Paper No. 152, 30 pp. (Available via the Internet at http://www.netl.doe.gov/publications/proceedings/06/carbon-seq/Tech%20Session%20152.pdf.)
76. United States Department of Labor, Occupational Safety and Health Administration. Hydrogen Sulfide, Hazards, https://www.osha.gov/SLTC/hydrogensulfide/hazards.html [accessed May 5, 2017].
77. *Occupational exposure to hydrogen sulfide.* Cincinnati, OH, US Department of Health, Education, and Welfare, 1977 (DHEW Publication (NIOSH) No. 77-158)
78. Hammer, G.; Lübcke, T.; Kettner, R.; Pillarella, M. R.; Recknagel, H.; Commichau, A.; Neumann, H.; Paczynska-Lahme, B. Natural Gas. Ullmann's Encyclopedia of Industrial Chemistry; Wiley-VCH Verlag GmbH & Co. KGaA: Weinheim, 2006.
79. Awe, O. W.; Zhao, Y.; Nzihou, A.; Minh, D. P.; Lyczko, N. A Review of Biogas Utilisation, Purification and Upgrading Technologies. Waste Biomass Valorization 2017, 8, 267-283.
80. U.S. Department of Energy, The National Energy Technology Laboratory. Gasification Introduction, Syngas Composition, https://www.netl.doe.gov/research/coal/energy systems/gasification/gasifipedia/syngas-composition [accessed May 5, 2017].
81. Emission Factor and Inventory Group, Office of Air Quality Planning and Standards. Petroleum Industry. Compilation of Air Pollutant Emission Factors. Vol. 1: Stationary

Point and Area Sources, AP- 42, 5th ed.; U.S. Environmental Protection Agency: Research Triangle Park, NC, January 1995; Chapter 5.

82. Gamson, B. W.; Elkins, R. H. Sulfur from Hydrogen Sulfide. Chem. Eng. Prog. 1953, 49, 203-215.
83. Pieplu, A.; Saur, O.; Lavalley, J.-C.; Legendre, O.; Ne´ dez, C.´ Claus Catalysis and H2S Selective Oxidation. Catal. Rev.: Sci. Eng. 1998, 40, 409-450.
84. Pandey, R. A.; Malhotra, S. Desulfurization of Gaseous Fuels with Recovery of Elemental Sulfur: An Overview. Crit. Rev. Environ. Sci. Technol. 1999, 29, 229-268.
85. Eow, J. S. Recovery of Sulfur from Sour Acid Gas: A Review of the Technology. Environ. Prog. 2002, 21, 143-162.
86. Mansi S. Shah, Michael Tsapatsis, and J. Ilja Siepmann Hydrogen Sulfide Capture: From Absorption in Polar Liquids to Oxide, Zeolite, and Metal-Organic Framework Adsorbents and Membranes, Chem. Rev. 2017, 117, 9755-9803
87. A.M. Ingallinella, V.A. Pacini, R.G. Fernández, R.M. Vidoni, G. Sanguinetti, Simultaneous removal of arsenic and fluoride from groundwater by coagulationadsorption with polyaluminum chloride, J. Environ. Sci. Health, Part A 46 (2011) 1288–1296.
88. M. Karatas, Removal of Pb(II) from water by natural zeolitic tuff: Kinetics and thermodynamics, J. Hazard. Mater. 199–200 (2012) 383–389.
89. A. Begum, M. Ramaiah, I. Harikrishna, K. Veena Khan, Heavy metal pollution and chemical profile of Cauvery River water, E.-J. Chem. 6 (2009) 47–52.
90. J. Liu, X. Wang, T. Xu, G. Shao, Novel negatively charged hybrids. 1. copolymers: Preparation and adsorption properties, Sep. Purif. Technol. 66 (2009) 135–142.
91. O.C.S.A. Hamouz, M.K. Estatie, M.A. Morsy, T.A. Saleh, Lead ion removal by novel highly cross-linked Mannich based polymers, J. Taiwan Inst. Chem. Eng. 70 (2017) 345–351.
92. S. Ramalingam, L. Parthiban, P. Rangasamy, Biosorption modeling with multilayer perceptron for removal of lead and zinc ions using crab shell particles, Arab. J. Sci. Eng. 39 (2014) 8465–8475.
93. D.M. Burke, M.A. Morris, J.D. Holmes, Chemical oxidation of mesoporous carbon foams for lead ion adsorption, Sep. Purif. Technol. 104 (2013) 150–159.

94. G. Edris, Y. Alhamed, A. Alzahrani, Biosorption of cadmium and lead from aqueous solutions by chlorella vulgaris biomass: equilibrium and kinetic study, Arab. J. Sci. Eng. 39 (2014) 87–93.
95. C. Dulcy Evangelin, S.G. Gunasekaran, M. Dharmendirakumar, Removal of lead ions from aqueous solutions by adsorption onto chemically modified silk cotton hulls by different oxidizing agents, Asia-Pac. J. Chem. Eng. 8 (2013) 189–201.
96. R. Song, D. Yang, L. He, Preparation of Semi-aromatic polyamide(PA)/multi-wall carbon nanotube (MWCNT) composites and its dynamic mechanical properties, J. Mater. Sci. 43 (2008) 1205–1213.
97. O.C.S. Al Hamouz, I.O. Adelabu, T.A. Saleh, Novel cross-linked melamine based polyamine/CNT composites for lead ions removal, J. Environ. Manage. 192 (2017) 163–170.
98. O.C.S. Al Hamouz, O.S. Akintola, Removal of lead and arsenic ions by a new series of aniline based polyamines, Process Saf. Environ. Prot. 106 (2017) 180–190.
99. O.C.S. Al Hamouz, S.A. Ali, Novel cross-linked polyphosphonate for the removal of Pb2+ and Cu2+ from aqueous solution, Ind. Eng. Chem. Res. 51 (2012) 14178–14187.
100. S. Wu, B. Duan, X. Zeng, A. Lu, X. Xu, Y. Wang, Q. Ye, L. Zhang, Construction of blood compatible lysine-immobilized chitin/carbon nanotube microspheres and potential applications for blood purified therapy, J. Mater. Chem. B 5 (2017) 2952–2963.
101. S. Akay, B. Kayan, D. Kalderis, M. Arslan, Y. Yagci, B. Kiskan, Poly(benzoxazine-cosulfur):An efficient sorbent for mercury removal from aqueous solution, J. Appl. Polym. Sci. 134 (2017) 45306–n/a.
102. T.A. Saleh, Isotherm, kinetic, and thermodynamic studies on Hg(II) adsorption from aqueous solution by silica- multiwall carbon nanotubes, Environ. Sci. Pollut. Res. 22 (2015) 16721–16731.
103. S. Yao, Z. Liu, Z. Shi, Arsenic removal from aqueous solutions by adsorption onto iron oxide/activated carbon magnetic composite, J. Environ. Health Sci. Eng. 12 (2014) 58.
104. R.S. Azarudeen, R. Subha, D. Jeyakumar, A.R. Burkanudeen, Batch separation studies for the removal of heavy metal ions using a chelating terpolymer: synthesis, characterization and isotherm models, Sep. Purif. Technol. 116 (2013) 366–377.

105. R. Subha, C. Namasivayam, vKinetics and isotherm studies for the adsorption of phenol using low cost micro porous ZnCl2 activated coir pith carbon, Can. J. Civ. Eng. 36 (2009) 148–159.
106. H.K. Boparai, M. Joseph, D.M. O'Carroll, Kinetics and thermodynamics of cadmium ion removal by adsorption onto nano zerovalent iron particles, J. Hazard. Mater. 186 (2011) 458–465.
107. E.I. Unuabonah, K.O. Adebowale, B.I. Olu-Owolabi, Kinetic and thermodynamic studies of the adsorption of lead (II) ions onto phosphate-modified kaolinite clay, J. Hazard. Mater. 144 (2007) 386–395.
108. C.-L. Hsueh, Y.-W. Lu, C.-C. Hung, Y.-H. Huang, C.-Y. Chen, Adsorption kinetic, thermodynamic and desorption studies of C.I. Reactive Black 5 on a novel photoassisted Fenton catalyst, Dyes Pigm. 75 (2007) 130–135.
109. Sahu, R.C., R. Patel, and B.C. Ray, Removal of hydrogen sulfide using red mud at ambient conditions. Fuel Processing Technology, 2011. 92(8): p. 1587-1592.
110. Plaza, M.G., et al., CO2 capture by adsorption with nitrogen enriched carbons. Fuel, 2007. 86(14): p. 2204-2212.
111. Chu, S., Carbon Capture and Sequestration. 2009. 325(5948): p. 1599-1599.
112. De Silva, P.N.K. and P.G. Ranjith, Understanding and application of CO2 adsorption capacity estimation models for coal types. Fuel, 2014. 121: p. 250-259.
113. Seul-Yi Lee, S.-J.P., A review on solid adsorbents for carbon dioxide capture. Journal of Industrial and Engineering Chemistry, 2015. 23: p. 1-11.
114. Yoosuk, B., T. Wongsanga, and P. Prasassarakich, CO2 and H2S binary sorption on polyamine modified fumed silica. Fuel, 2016. 168: p. 47-53.
115. Meth, S., et al., Silica Nanoparticles as Supports for Regenerable CO2 Sorbents. Energy & Fuels, 2012. 26(5): p. 3082-3090.
116. Abdouss, M., et al., Effect of the structure of the support and the aminosilane type on the adsorption of H2S from model gas. RSC Advances, 2014. 4(12): p. 6337-6345.
117. Li, Y., et al., Adsorption separation of CO2/CH4 gas mixture on the commercial zeolites at atmospheric pressure. Chemical Engineering Journal, 2013. 229: p. 50-56.

118. Abdelnaby, Mahmoud M., et al., Carbon dioxide capture in the presence of water by an amine-based crosslinked porous polymer. Journal of Materials Chemistry A, 2018. 6(15): p. 6455-6462.
119. Jeon, H.J., et al., Highly Selective CO2-Capturing Polymeric Organic Network Structures. 2012. 2(2): p. 225-228.
120. Xu, Y., et al., Light-Emitting Conjugated Polymers with Microporous Network Architecture: Interweaving Scaffold Promotes Electronic Conjugation, Facilitates Exciton Migration, and Improves Luminescence. Journal of the American Chemical Society, 2011. 133(44): p. 17622-17625.
121. Luo, Y., et al., Hypercrosslinked Aromatic Heterocyclic Microporous Polymers: A New Class of Highly Selective CO2 Capturing Materials. 2012. 24(42): p. 5703-5707.
122. Fila, K., et al., Thermal and spectral analysis of copolymers with sulphur groups. 2018. 133(1): p. 489-497.
123. Wood, C.D., et al., Hydrogen Storage in Microporous Hypercrosslinked Organic Polymer Networks. Chemistry of Materials, 2007. 19(8): p. 2034-2048.
124. Deng, H., et al., Large-pore apertures in a series of metal-organic frameworks. Science, 2012. 336(6084): p. 1018-23.
125. Arab, P., et al., Copper(I)-Catalyzed Synthesis of Nanoporous Azo-Linked Polymers: Impact of Textural Properties on Gas Storage and Selective Carbon Dioxide Capture. Chemistry of Materials, 2014. 26(3): p. 1385-1392.
126. Thommes, M., Physisorption of gases, with special reference to the evaluation of surface area and pore size distribution (IUPAC Technical Report), in Chemistry International. 2016. p. 25.
127. Wilmer, C.E., et al., Structure–property relationships of porous materials for carbon dioxide separation and capture. Energy & Environmental Science, 2012. 5(12): p. 9849-9856.
128. Li, P.-Z. and Y. Zhao, Nitrogen-Rich Porous Adsorbents for CO2 Capture and Storage. 2013. 8(8): p. 1680-1691.
129. İslamoğlu, T., M. Gulam Rabbani, and H.M. El-Kaderi, Impact of post-synthesis modification of nanoporous organic frameworks on small gas uptake and selective CO2 capture. Journal of Materials Chemistry A, 2013. 1(35): p. 10259-10266.

130. Llewellyn, P.L. and G. Maurin, Gas adsorption microcalorimetry and modelling to characterise zeolites and related materials. Comptes Rendus Chimie, 2005. 8(3): p. 283-302.
131. Jensen, A.B. and C. Webb, Treatment of H2S-containing gases: A review of microbiological alternatives. Enzyme and Microbial Technology, 1995. 17(1): p. 2-10.
132. Saha, A.K., et al., Selective removal of hydrogen sulfide from gases containing hydrogen sulfide and carbon dioxide by absorption into aqueous solutions of 2-amino-2-methyl-1-propanol. Industrial & Engineering Chemistry Research, 1993. 32(12): p. 3051-3055.
133. Das, A., et al., The H2S Dimer is Hydrogen-Bonded: Direct Confirmation from Microwave Spectroscopy. 2018. 57(46): p. 15199-15203.
134. Huang, K., et al., Absorption of H2S and CO2 in Aqueous Solutions of Tertiary-Amine Functionalized Protic Ionic Liquids. Energy & Fuels, 2017. 31(12): p. 14060-14069.
135. Liu, C., et al., Selective removal of H2S from biogas using a regenerable hybrid TiO2/zeolite composite. Fuel, 2015. 157: p. 183-190.
136. Fauteux-Lefebvre, C., et al., Carbon Nanofilaments Functionalized with Iron Oxide Nanoparticles for in-Depth Hydrogen Sulfide Adsorption. Industrial & Engineering Chemistry Research, 2015. 54(37): p. 9230-9237.
137. Balsamo, M., et al., ZnO-CuO supported on activated carbon for H2S removal at room temperature. Chemical Engineering Journal, 2016. 304: p. 399-407.
138. Rezaei, S., et al., Novel Copper-Exchanged Titanosilicate Adsorbent for Low Temperature H2S Removal. Industrial & Engineering Chemistry Research, 2012. 51(38): p. 12430-12434.

Vitae

Name	:Muhammad Alasad Albakri
Nationality	:Syrian
Date of Birth	:4/2/1984
Email	:malbakri84@yahoo.com
Address	:Saudi Arabia – Khobar City
Academic Background	:MSc in Chemistry

Publications:

- ✓ New series of benzene-1,3,5-triamine based cross-linked polyamines and polyamine/CNT composites for lead ion removal from aqueous solutions, chemical engineering journal.